Timing and controls on the delivery of coarse sediment to deltas and submarine fans on a formerly glaciated coast and shelf

Alexandre Normandeau[1,2], Pierre Dietrich[3,4], Patrick Lajeunesse[2], Guillaume St-Onge[5], Jean-François Ghienne[3], Mathieu J. Duchesne[6] and Pierre Francus[7]

[1] *Geological Survey of Canada – Atlantic, 1 Challenger Drive, Dartmouth, Nova Scotia, B2Y 4A2, Canada*

[2] *Centre d'études nordiques & Département de géographie, Université Laval, 2405 Rue de la Terrasse, Québec, Québec G1V 0A6, Canada*

[3] *Institut de physique du Globe de Strasbourg, UMR 7516 CNRS/Université de Strasbourg, 1 rue Blessig, 67084 Strasbourg, France*

[4] *Department of Geology, Auckland Park Kingsway Campus, University of Johannesburg, Johannesburg, South Africa*

[5] *Institut des sciences de la mer de Rimouski, Canada Research Chair in Marine Geology & GEOTOP, Université du Québec à Rimouski, 310 Allée des Ursulines, Rimouski, Québec, G5L 3A1, Canada*

[6] *Geological Survey of Canada – Québec, 490 rue de la Couronne, Québec, Qc. G1K 9A9, Canada*

[7] *Institut national de la recherche scientifique, Centre Eau Terre Environnement, & GEOTOP, 490 rue de la Couronne, Québec, Qc. G1K 9A9, Canada*

ABSTRACT

The evolution of deltas and submarine fans is often envisioned as largely controlled by relative sea-level (RSL) variations. However, in some cases, RSL can have less effect on delta and submarine fan activity than sediment supply and shelf geomorphology. In order to document the relative importance of these three factors on deltaic and submarine fan evolution in a former glaciated environment, this paper documents the delivery of coarse sediment to the Laurentian Channel (eastern Canada). The well-constrained stratigraphic and geomorphological framework of both the glacio-isostatically uplifted deltas and the modern Laurentian Channel fans allow us to document and contrast the evolution of river-fed deltas, river-fed canyon/fan systems and longshore drift-fed fans during deglacial and postglacial times. The evolution of these different types of fans can be divided into three phases. The first phase is characterized by delta progradation on the shelf while RSL was at its maximum, although already falling, and the ice-margin gradually retreated inland. The second phase is characterized by the delivery of deltaic sediment in the deep realm of the Laurentian Channel, permitted by the supply of large amounts of glaciogenic sediments derived from the retreating ice margin and the lowering of the RSL. At the same time, sediment instability along the steep Laurentian

Channel formed small incisions that evolved into submarine canyons where the narrow shelf allowed the trapping of longshore sediment. The third phase is characterized by the withdrawal of the ice-margin from the watershed of the main rivers and the drastic decrease in sediment supply to the deltas. Consequently, the delta fronts experienced strong coastal erosion, even though RSL was still lowering in some cases, and the eroded sediments were transferred onto the shelf and to adjacent bays. This transfer of coastal sediments allowed the continued activity of longshore drift-fed canyons. The retreat of the ice margin from the watersheds thus controlled the supply of sediment and induced a change in delta type, passing from river-dominated to wave-dominated. This paper highlights the role of the type of sediment supply (ice-contact, glaciofluvial and longshore drift) in the timing and activity of submarine fans in high-latitude environments. It proposes a conceptual model for high-latitude shelves where sediment delivery to submarine fans is mostly controlled by structural inheritance (watershed area and shelf geomorphology) rather than RSL fluctuations. Therefore, although RSL fell during delta progradation, this study demonstrates that it was not the main contributor to delta and submarine fan growth. This has wider implications for the extraction of sea-level information from stratigraphic successions.

INTRODUCTION

Deltas and submarine fans are the main depositional systems accumulating terrigenous sediments originating from sediment density flows (sensu Talling et al., 2012). Deltas are associated with a river source whereas submarine fans can be connected to submarine canyons fed either by rivers (e.g., Babonneau et al., 2013), longshore drift (e.g., Lewis

and Barnes, 1999) or glacial meltwaters (e.g., Roger et al., 2013). Deltas and fans of limited extent can be observed in shallow waters, such as at the head of fjords (Prior and Bornhold, 1989; Conway et al., 2012; Hughes Clarke et al., 2014) and on coastal shelves (Normandeau et al., 2013; Warrick et al., 2013), providing a great opportunity for documenting sediment transport using very high-resolution mapping techniques (e.g., Hill, 2012; Hughes Clarke et al., 2014; Normandeau et al., 2014). These shallow water systems can then serve as high-resolution analogues to larger deep-water systems and improve our overall understanding of sediment density flow processes and timing in relation to sediment supply and relative sea-level (RSL).

The architecture of deltas and submarine fans is usually envisioned as largely controlled by RSL variations, where forced regressions lead to fast progradation into marine basins. However, the architecture and activity of deltas and submarine fans are known not only to be controlled by RSL, but also by tectonic settings, climatic conditions and grain-size (Bouma, 2004). RSL variations exert a major control on the activity of deltaic and turbidite systems (Porębski and Steel, 2003; Covault and Graham, 2010; Paull et al., 2014) where, at sea-level lowstands, continental sediments are easily transported to continental margins, while in sea-level highstands, sediments are trapped in estuaries (e.g., Maslin et al., 2006). However, these models were developed for passive margins with broad shelves where continental sediment supply is relatively constant over time. Such models lead to false interpretations where tectonic settings favour a direct link between coastal sediments and deep-sea settings (Migeon et al., 2006; Covault et al., 2007; Boyd et al., 2008; Romans et al., 2009; Babonneau et al., 2013) or where climatic

85 conditions favour high sediment discharges from rivers (Ducassou et al., 2009; Rogers
86 and Goodbred, 2010).

87 In glacio-isostatically uplifted shelves, the study of deltas and submarine fans is often
88 restricted to either their modern exposed component (i.e., outcrops: Corner, 2006;
89 Eilertsen et al., 2011; Marchand et al., 2014; Nutz et al., 2015) or to their modern
90 submarine component (submarine deltas: e.g., Sala and Long, 1989; Normandeau et al.,
91 2015). In these settings, since sediments composing the deltas were deposited below sea-
92 level and subsequently glacio-isostatically uplifted in part above sea-level, both the
93 modern exposed and marine components should be studied as a whole rather than
94 separately. The study of deltas and submarine fans is incomplete without taking into
95 account both their exposed and marine components. In this respect, the variety of types of
96 deltas and submarine fans located in the Lower St. Lawrence Estuary (LSLE) provide
97 ideal sites to examine deltaic progradation and submarine fan deposition in a glacio-
98 isostatically uplifted setting.

99 While most of the uplifted deltas and fans of the LSLE have been studied inland
100 (Bernatchez, 2003; Marchand et al., 2014; Dietrich et al., 2016a; in press), the links
101 between them and their submarine counterparts in the Laurentian Channel have never
102 been thoroughly examined. These systems vary greatly in size, morphology and sediment
103 sources (Normandeau et al., 2015). Four major types of submarine canyons and channels
104 were described in the LSLE, using a source-based classification: 1) river-fed channels; 2)
105 longshore drift-fed canyons; 3) glacially-fed canyon; and 4) sediment-starved canyons
106 (Fig. 1; Normandeau et al., 2015). The modern activity of these channels and canyons

was shown to be dependent on their slope since sediment supply is today low at the head of these systems. However, their evolution in relation to sediment supply, RSL change and shelf geomorphology has not been addressed. Documenting the evolution of such different systems in a confined area allows determining the major controls over sediment transport processes in a formerly glaciated margin.

The extensive high-resolution bathymetric datasets and the time-constrained seismostratigraphic framework of the LSLE offer an excellent opportunity to document: 1) the type and chronology of sediment density flows related to the different types of deltas and submarine fans in a formerly glaciated margin and in a forced regression setting; and 2) the factors controlling delta progradation and submarine fan deposition in relation to sediment supply, shelf geomorphology and RSL change. This paper thus reports on the variability, timing and frequency of late-Quaternary delta and submarine fan activity in the LSLE in relation to their geological evolution by using new seismic and sedimentological data and synthesizing previous studies in the LSLE.

PHYSICAL SETTING

The Laurentian Channel forms a deep (>300 m) and long (1500 km) submarine trough in the St. Lawrence Estuary and Gulf that extends from Tadoussac to the edge of the North Atlantic continental shelf (Fig. 1). It is bordered by 0-20 km-wide coastal shelves (Pinet et al., 2011) bounded by generally steep slopes (2-20°). The coastal shelves lead landward to a series of emerged and gently sloped hills reaching few hundreds of meters in elevation. Inland, the bedrock is deeply incised (100-400 m) by steep-flanked,

normally-oriented structural valleys, 0.5-3 km in width, their bottom lying between 50 m above sea level and 300 m below sea level (Lajeunesse, 2014).

The chronology of deglaciation in the LSLE was marked by four stages of glacial retreat of the Laurentide Ice Sheet (LIS) (see Shaw et al. (2006) and Occhietti et al. (2011)). Before 23.5 ka cal BP, while the LIS margin at times reached the edge of the North Atlantic continental shelf (Shaw et al., 2006), the ice thickness over the Gulf of St. Lawrence was greater than 1500 m (Marshall et al., 2000; Tarasov et al., 2012). By 14.8 ka cal BP, iceberg calving at the margin of the LIS led to its rapid retreat through the Laurentian Channel until it reached the Tadoussac region (Shaw et al., 2006). During the Younger Dryas cold episode (13-11.7 ka cal BP), the LIS margin mainly stabilized offshore (St-Onge et al., 2008) (Fig. 2). At that time, Pointe-des-Monts was the only ice-free sector of the Québec North Shore (Occhietti et al., 2011). This stabilization resulted in the deposition of grounding-zones wedges in the LSLE (Lajeunesse, 2016). Following the Younger Dryas cold episode, the LIS margin retreated inland due to climate warming starting at 11.7 ka cal BP. This stage is characterized by terrestrial melting of the LIS (Occhietti et al., 2011); the inland retreat being slower than in the second glaciomarine stage (Shaw et al., 2006). The North Shore watershed was entirely deglaciated by *ca*. 7 ka cal BP (Fig. 2).

Directly following the deglaciation of the study area, the RSL reached *ca.* 150 m in altitude (marine limit) over the entire North Shore region due to the deglacial Goldthwait Sea invasion of the glacio-isostatically flexured land (Occhietti et al., 2011). Large areas of the now-emerged land were thus flooded at that time, including the bottom of the

150 structural valleys that then formed fjords. The glacio-isostatic adjustment led to a RSL
151 fall that reached 2 to 4 $cm.yr^{-1}$ in spite of the concomitant global eustatic rise (Boulton,
152 1990; Tarasov et al., 2012, Peltier et al., 2015; Dietrich et al., 2016b). Most often, deltaic
153 systems fed by glaciofluvial rivers were initially confined within the fjords prior to their
154 emergence on the coastal shelf. RSL fall led to a drastic reduction of the width of the
155 coastal shelf and in places to its complete emergence.

156 The retreat of the LIS over the LSLE led to a thick sediment accumulation (> 400 m) in
157 the Laurentian Channel (Syvitski and Praeg, 1989; Josenhans and Lehman, 1999;
158 Duchesne et al., 2010). Duchesne et al. (2010) distinguished five main seismic units (SU)
159 composing this Quaternary infill (Fig. 3), in addition of three secondary units observed
160 sporadically in the LSLE succession. SU1 may consist of thin till layers or patches, but
161 could also be composed of reworked pre-Wisconsinan sediments. SU2 was analyzed in
162 detail by St-Onge et al. (2008) and was interpreted as ice-proximal to ice-distal sediments
163 deposited during the rapidly retreating LIS margin in the LSLE. The deposition of this
164 unit occurred before 11 ka cal BP. Massive clay composes SU3 and was deposited when
165 the ice margin was located inland (Duchesne et al., 2010), between *ca.* 11 ka cal BP and
166 *ca.* 8.4 ka cal BP. SU4 and SU5 are composed of postglacial hemipelagic sediments
167 deposited since *ca.* 8.4 ka cal BP. SU6 and SU7 represent submarine fans and mass
168 movement deposits that are located near river mouths and on steep slopes (Pinet et al.,
169 2011). While SU1 to SU5 correspond to a stratigraphic succession (from the lowest and
170 oldest to shallowest and youngest), SU6 and SU7 correspond to sedimentary bodies that
171 were deposited within the previous units. Finally, SU8 consists of a contourite deposit

located near the head of the Laurentian Channel (Duchesne et al., 2010). Today, sediments composing the Laurentian Channel seafloor mainly originate from the Québec North Shore (Jeagle, 2014) where rivers have larger watersheds than on the South Shore.

METHODOLOGY

Data and methods

Modern exposed component (outcrop)

Internal stratigraphic architecture and sedimentological content of the modern exposed component of the deltaic systems were investigated along cliffs and river banks that expose the strata. Regularly spaced sedimentary sections (1:100 scale) were logged and correlated with the help of photomosaics, in order to produce a detailed stratigraphic framework (e.g., Dietrich et al., in press). Depositional environments were deduced from both the stratigraphic architecture and sedimentological content and followed the well-documented history of RSL fall in deglacial and postglacial times (Dionne, 2001; Shaw et al., 2002; Tarasov et al., 2012). Radiocarbon dating of marine shells and plant debris sampled almost exclusively in mud-rich strata constrain the chronostratigraphic framework of the deltaic development.

Modern submarine component (multibeam and seismic surveys)

Seismic profiles were acquired using an Applied Acoustics Squid 2000 sparker system (2 kJ, *ca.* 500 Hz peak frequency, 0.75 m vertical resolution) deployed from the R/V Coriolis II in 2012. They were analyzed and visualized using the Geological Survey of Canada *SEGYJP2* software. Piston (PC) and gravity (TWC) cores were collected during

193 the 2006 and 2012 cruise on board R/V Coriolis II. Cores were first analyzed through a
194 *Siemens Somatom Volume Sensation* CT-Scan (97 x 97 x 400 microns/voxel, 0.4 mm
195 thick slice). The CT-Scan allowed a non-destructive visualization of longitudinal and
196 transverse sections of cores using X-ray attenuation. Grey levels vary according to the
197 density, mineralogy and porosity of sediments (St-Onge et al., 2007; Fortin et al., 2013)
198 and allow recognizing sedimentary structures and establishing a high-resolution
199 stratigraphy (St-Onge and Long, 2009). Following this operation, the cores were opened,
200 described and photographed. Magnetic susceptibility was then measured using a Geotek
201 Multi-Sensor Core Logger (MSCL) at 0.5 cm intervals. Grain-size analyses were
202 performed using a *Beckman Coulter^{TM} LS13320 laser sizer* or a *Horiba laser sizer* at 10
203 cm intervals on background sediment and at 1-2 cm intervals on selected facies.
204 Sediments were diluted into a calgon solution for at least 3 hours and shaken, then
205 disaggregated to an ultrasonic bath. At least three runs were averaged. Statistical
206 parameters were obtained using Gradistat (Blott and Pye, 2001). Thin sections were made
207 from on selected facies and were used to extract grain-size information following Francus
208 (1998) and Francus and Nobert (2007). These grain-size results were shown to be
209 comparable to the laser diffraction technique for unimodal distributions.

210 Accelerator mass spectrometry (AMS) ^{14}C dating was performed on the cores from
211 organic matter and shell remains (Table 2).Radiocarbon ages, sampled both in exposed
212 and submarine delta components, were converted to calendar ages using the Calib 7.0
213 program (Stuiver and Reimer, 1993) with the Reimer et al. (2013) Marine13 dataset. The
214 Marine13 dataset applies a reservoir correction of 400 years (ΔR – 0 yr), which is in

agreement with reservoir ages for the LSLE during the last 7.7 ka ^{14}C BP (St-Onge et al., 2003).

Study site justification

The paleogeographical reconstruction presented here focuses on deltas and fans that are documented with extensive seismic and sedimentological datasets (Fig. 1). Therefore, data from the modern exposed component of the Portneuf delta described in Dietrich et al. (in press) is used as an example for the evolution of deltas on the shelf. This cross-section is considered representative of all of the exposed deltas in the LSLE (e.g., Bernatchez, 2003) as the whole area experienced a similar history of ice margin retreat and RSL fall.

In the modern submarine component, we document newly recovered data from the Manicouagan delta. The Manicouagan delta is considered as having had the most long-lived glacier-related sedimentation of all the deltas in the LSLE because of the size and extent of its drainage basin that permitted a perennial connection with the northward retreating LIS margin (Dietrich, 2015) (Fig. 2). This glaciogenic sedimentation longevity is reflected today by the size of the Manicouagan delta, which is the largest of all the deltas in the LSLE. This delta can thus be convincingly used as an end-member of the activity of river-fed deltaic submarine fans.

The Pointe-des-Monts canyons (Fig. 1; Normandeau et al., 2014) were ignored in this analysis because they lack sediment supply at their heads. The goal of this paper is to examine the links between sediment supply, RSL and shelf geomorphology. Since the

236 Pointe-des-Monts canyons do not respond to typical external forcings, they are unique
237 and are studied separately in other papers (Normandeau et al., 2014, 2015).

238 **RESULTS AND INTERPRETATIONS**

239 **Modern exposed component of the deltaic systems**

240 The modern exposed component of the studied deltaic systems mainly consist of large
241 (tens to hundreds of km²) sedimentary bodies protruding in the LSLE, emplaced at the
242 immediate outlet of structural valleys (Dietrich et al., in press). This sedimentary
243 succession is now exposed due to RSL fall forced by the glacio-isostatic rebound but
244 originally prograded on the shelf. Today, these deltas lack evidence of river-fed
245 progradation; they rather experience shoreline retreat (Bernatchez and Dubois, 2004) or
246 longshore-drift related accretion (Normandeau et al., 2015). In places, the shoreline
247 retreat allows the observation of their internal stratigraphic architecture. These deltaic
248 bodies are several tens of meters in thickness and consist of three main laterally
249 juxtaposed or vertically superimposed architectural elements (Dietrich et al., in press): 1)
250 outwash fans and glaciomarine mud; 2) glaciofluvial deltas; and 3) coastal suites (Fig.
251 4A).

252 ***Outwash fans and glaciomarine mud***

253 Outwash fans form 20-60 m-thick sediment wedges and generally constitute the core of
254 the exposed component of the deltaic system. These wedges are characterized by flat
255 topsets and basinward-dipping clinothems. The topsets, lying at or immediately below the
256 marine limit, consist of very coarse-grained materials (sand to boulders) and m-sized

sand intraclasts characterized by faint horizontal bedding and occasional trough cross-strata (Fig. 4B). Aerial photographs reveal the presence of relict kettle holes and inactive braided channels on the topsets. Clinothems are essentially composed of sand 5 km away from the fan apex, and grade distally into silty material (>10 km away from the apex). Highly channelized, massive, normally-graded sand beds are ubiquitous (Fig. 4C). These beds are interpreted as being deposited by channelized debris flows and high-density sediment density flows respectively (Talling et al, 2012). Downslope, silty material consists of finely-laminated silt beds and fine-grained sand interbeds forming pluri-m successions. Cm-sized lonestones, interpreted as ice-rafted debris (IRD), are scattered within the silt beds. These silt and sand beds are interpreted as being deposited by low-density sediment density flows (Talling et al., 2012) in a glaciomarine environment. A discontinuous silt veneer (1 to 10 m-thick) with abundant IRD, up to boulder-sized, underlies the entire sediment wedge and drapes the underlying bedrock (Fig. 4D). Shell fragments sampled in this sandy to silty sediment wedge provided ages of 11 170 ± 70, 11 500 ± 100 and 12 250 ± 150 cal BP (Dietrich et al., 2016a).

The proximal coarse to very-coarse sediment size that distally evolves into fine-grained facies, the presence of relict kettle holes and braided channels on the apex of the sediment wedges, the presence of IRDs in mud, relatively ancient radiocarbon ages and inferred high RSL (marine limit) altogether indicate that these sedimentary bodies were emplaced in an ice-contact outwash fan during the Younger Dryas cold episode. Triggering processes of sediment density flows that deposited normally-graded beds observed throughout the depositional slopes can be the collapse of the delta lip or alternatively the

direct plunging of hyperpycnal underflows derived from the nearby ice-margin. Tidal processes also likely played an important role in modulating sediment density flow events that permitted the deposition of cyclically-laminated layers but also probably in initiating supercritical flow events (tidal-drawdown process, Smith et al., 1990; Dietrich et al., 2016a).

Glaciofluvial deltas

Glaciofluvial deltas are related to extensive landforms located at or near the outlet of the structural valleys, immediately basinward of the outwash fans. Landforms left by glaciofluvial deltas, once commonly protruding in the LSLE, have their top dipping gently toward the basin and lying at elevations well below marine limit (between 150 and 40 m asl). These sediment bodies reach ≥ 70 m in thickness and can be identified by their well-defined tripartite architecture formed by topset, foreset and bottomset beds, interpreted as delta plain, delta slope and prodelta deposits, respectively (Fig. 4). The delta plain is composed of a ≤ 10 m-thick sand and gravel sheet with trough and planar cross-strata (Fig. 4E) emplaced in braided fluvial channels, some of which are observed in plan-view. The delta plain discordantly overlies the delta slope deposits. The tens of m-thick delta slope deposits are formed of seaward-dipping (average of 6°, up to 17° in places) sand beds. The latter are normally-graded, erosion-based and formed of T_b, T_c, flamed T_e and frequent basal T_a intervals including lithic and rip-up clasts (Fig. 4F). These beds are interpreted as being deposited by recurrent high-density sediment density flows (Talling et al., 2012), commonly supercritical as indicated by T_a intervals (Postma et al., 2009). The triggering mechanisms of these sediment density flow events, whether

301 they were hyperpycnal or induced by the collapse of the delta lip, cannot be clearly
302 defined. Sand beds grade downward into gently sloped (<1°) and well-bedded silty
303 facies, indicative of prodeltaic sedimentation (Fig. 4G). These facies that consist of an
304 alternation between silt beds and sand interbeds are interpreted as deposited by low-
305 density sediment density flows (Talling et al., 2012) and/or by settling from an overlying
306 sediment-laden buoyant plume. Inverse grading has been observed in X-ray in silt beds
307 possibly suggesting hyperpycnal flows (e.g., Mulder et al., 2003). Radiocarbon dating
308 performed on shells sampled in silt beds provided ages of 9 370 ± 100, 9 535 ± 15, 10
309 210 ± 25, 10 415 ± 145, 10 420 ± 140 and 10 600 ± 115 cal BP. Radiocarbon dates
310 sampled in these glaciofluvial deltas and those found in the underlying outwash fan
311 indicate that the deltaic systems prograded rapidly at rates between 10 and 20 $m.yr^{-1}$
312 (Dietrich et al., in press).

313 As they were emplaced basinward of the outwash fans, during periods when RSL was
314 significantly lower than marine limit –although higher than modern sea level–, the deltas
315 of the North Shore of the LSLE are interpreted as being fed by glaciofluvial rivers
316 delivered from the nearby but retreating land-based LIS margin (Duchesne et al., 2010;
317 Dietrich et al., in press). The large amount of meltwater and clastic sediment supplied to
318 the deltas is evidenced by: 1) high progradation rates; 2) the prevalence of beds deposited
319 by sediment density flows, including those from supercritical flows; 3) the relict braided
320 fluvial pattern; and 4) the well-defined tripartite deltaic architecture (e.g., Swenson et al.,
321 2005). The spatial extent of these deltas showed that some of them prograded over the
322 entire width of the coastal shelf up to the shelf break. The presence of these deltas at the

outlets of structural valleys provides evidence that the latter efficiently drained to the LSLE meltwater effluents from the retreating LIS margins.

Coastal suites

The top of the glaciofluvial deltas, commonly located at elevations between 150 and 40 m asl (90 m asl in the case of the Portneuf delta), is characterized by a continuous, stepped and thin (1-5 m) sand veneer. This sand veneer, lying discordantly over the underlying glacio-fluvial delta slope, consists in its upper part of very well-sorted, well-laminated and occasionally bioturbated sand and heavy mineral placers (Fig. 4H) and in its lower part of gravel and pebble conglomerates underlied by a basal lag. Well-defined relict coastal landforms are visible on the top of this sand veneer, forming raised and stepped beaches and spits (Fig. 4I). The sand veneer is thus interpreted as a nearshore sand sheet including swash-backswash and surf zone deposits, for the upper and lower part respectively (Dietrich et al., in press). Thick sand-prone deposits (20 m) associated with the nearshore sand sheet have been observed where the underlying glaciofluvial delta slope deposits are thin and distinctively characterized by steep-sloped (up to 12°) and composite clinothems (Fig. 4A). These clinothems, composed of trough and sigmoidal cross-strata showing transverse paleo-flows compared to the master bed dips, constitutes a spit platform, over which the nearshore sandsheet prograded (Dietrich et al., in press). No datable material was found in these sand-prone deposits, neither in the nearshore sand sheet nor in the spit platform. Nevertheless, ages of deposition were inferred from the altitude of stepped paleo-shorelines by using local RSL curves (e.g., Shaw et al., 2002; Dietrich et al., in press). The highest paleo-shorelines were observed at

90 m asl in the Portneuf area (Fig. 4), indicating that the onset of the development of beach-related deposits occurred, in this particular deltaic system, at *ca.* 10 ka cal BP. Beach ridges and shorelines developed afterward in a stepped manner as RSL was rapidly falling owing to the post-glacial glacio-isostatic rebound.

Modern submarine component of the deltaic systems

The modern submarine component of the deltaic systems (SU6 of Duchesne et al., 2010) form the offshore counterpart of the modern exposed component described above, off the mouth of large rivers and valleys of the LSLE. Submarine fans are either on the shelf of the Laurentian Channel, where they are almost completely buried with a surface expression that is greatly reduced (e.g. the Portneuf submarine channels, Fig. 5A), or on the Laurentian Channel slope and basin where they are well- or better preserved (e.g. the Manicouagan submarine channels, Fig. 5B). A seismic profile collected over the Portneuf submarine channels reveals that a thick sediment accumulation overlies the main submarine fan unit (SU6; Fig. 6A). Additionally, the entire fan unit (SU6) is located within SU3, which indicates that the fan stopped being active prior to *ca.* 8.4 ka cal BP (transition SU3 to SU4) and 9.4 ka cal BP (age of middle of SU3; Duchesne et al., 2010), which confirms previous interpretations of the reduced deltaic progradation by 10 ka cal BP. A more detailed analysis of the Manicouagan submarine delta, in the Laurentian Channel, is presented here since its activity lasted longer. The analysis of the submarine deltaic deposits reveals that they are composed of three superimposed seismic units (SU, Fig. 6B): the bottomset beds, the main submarine fan and an hemipelagic sediment drape.

Bottomset beds

The lowermost unit, named SU3 and interpreted as ice-distal mud, is predominantly transparent on the seismic reflection data (Fig. 6B) and composed of massive clays (Duchesne et al., 2010). It drapes the underlying units and its thickness decreases gradually from West to East (Duchesne et al., 2010). In the Manicouagan region, these deposits are the bottomset beds (or prodelta). These sediments were deposited while the essentially sandy counterpart of the deltas, expressed by the modern exposed component, was prograding onto the shelf.

Deltaic submarine fans in the Laurentian Channel

As the delta reached the shelf edge as a result of active progradation and lowering of the RSL, deltaic sediments began to be delivered directly into the Laurentian Channel and the main submarine fans formed (SU6; Duchesne, 2005). The submarine fans have a wedge-shaped geometry and downlap the underlying SU3. In the Manicouagan delta, the submarine fans reach a thickness of *ca.* 50 m and consist of parallel to chaotic, medium to high amplitude seismic reflections (Fig. 6B). These chaotic reflections are interpreted as being the result of sediment density flows, namely debris flows originating from delta-lip failures while the parallel high-amplitude reflections are interpreted as resulting from river-derived density flows. The main submarine fan unit is located above SU3 and four channels are visible in the top-half of the seismic sequence (Fig. 5B-6B), with a conspicuous surface expression. These deposits are similar in geometry and facies to the deposits described earlier in the modern exposed component of the delta slope deposits (see section 4.1.2).

Four cores were collected on the Manicouagan submarine fan in order to constrain the final stages of fan deposition (Fig. 7). These sediment cores penetrated sediment density flow deposits at 4 m depth. These deposits consist of medium sand to coarse silt (20-200 µm) including coarsening-then-fining upward layers (Fig. 7E). They are generally thin (≤ 15 cm) and preserved parallel to wavy laminations. Their basal contact is generally sharp and erosive, and more rarely gradual. Several different types of grading patterns are observed within this facies. In core 23PC, a particular bed reveals more complex grading patterns, with stacked coarsening-to-fining upward layers or stacked normally graded layers (Fig. 7E). Their fine nature, the grain-size variability, the presence of fine laminations and their location off river mouths differentiate them from classical turbidites; they are therefore interpreted as river-derived sediment density flow deposits similar to the hyperpycnites of Mulder et al. (2003). Talling (2014) described fine-grained and very thin (mm to cm) deposits to be the result of hyperpycnal flows. The fine-grained and thin nature of the deposits are likely due to relatively slow moving and dilute flows. Hyperpycnal flows can result in inverse-to-normal grading (e.g., Mulder et al., 2003), but also in more complex grading patterns characterized by stacked inverse-to-normal or stacked normal grading (e.g., Lamb and Mohrig, 2009). Direct observations also showed that hyperpycnal flows can generate multiple pulses during a single flood (Khripounoff et al., 2009). It is however unclear how river-derived sediment density flow are triggered in this case, whether they directly plunge (hyperpycnal flow) or are related to the continuous settling from the river plume where sediment concentration is eventually sufficient to initiate turbidity currents with multiple pulses (Clare et al., 2016).

All of the cores collected on the Manicouagan fan contain series of hyperpycnite-like deposits. The base of core 16 PC is composed of four hyperpycnite-like deposits. Shell fragments and organic matter collected at 41 cm and 561 cm provided ages of 1800 ± 70 cal BP (UCIAMS-127443) and 6970 ± 90 cal BP (UCIAMS-127426) respectively. These two ages give an approximate sedimentation rate of *ca.* 0.096 cm/y for the postglacial sediments in this region. Core 17PC contains six hyperpycnite-like deposits near its base but the coring process led to the deformation of these facies. Shells fragments collected at 170 cm provided an age of 6300 ± 75 cal BP (UCIAMS-127454). In core 23PC, an hyperpycnite-like deposit is present at 750 cm near the base of the core and a very thin one (< 1 cm thick) is present at 350 cm. Shell fragments collected at 324 cm provided an age of 5530 ± 60 cal BP (UCIAMS-127444). Core 39PC contains three sediment density flow deposits that were identified between 0 and 550 cm. These deposits were disturbed due to the coring process and could either represent hyperpycnite-like deposits or classical turbidites. Three shell samples were collected for radiocarbon dating between 0 and 150 cm. The topmost sample, at 8 cm, provided an age of 5750 ± 160 cal BP (TO-13204). This age is likely inaccurate because two other dates on shell fragments collected at 91 cm and 126 cm provided ages of 1920 ± 135 cal BP (TO-13206) and 1150 ± 115 cal BP (TO-13205), respectively. Based on sedimentation rates of 0.046 cm/yr calculated from the two dates obtained, the hyperpycnite-like deposits observed in core 39PC approximately date to 4 ka cal BP, while the deposits in the other cores are generally older than 7 ka cal BP.

Hemipelagic sedimentation

Low amplitude seismic reflections drape the underlying Manicouagan submarine fan unit. These low amplitude reflections are composed of homogeneous fine to very fine silts (Fig. 7) and are interpreted as the result of the sedimentation of hemipelagic material. These sediments were essentially deposited over the sediment density flow deposits described above and are thus younger than 7 ka cal BP in the Manicouagan region. In other regions where deltaic activity ceased earlier, they can be as old as 10 ka cal BP over the submarine deltas. These hemipelagic sediments were thus deposited while coastal suites identified onshore were being constructed on the deltas near the coast (see section 4.1.3).

Laurentian Channel submarine canyons/fans

The submarine fans described in this section are unrelated to deltaic progradation and are rather related to river-fed and longshore drift-fed submarine canyons.

River-fed submarine canyon/fan

The river-fed submarine fan located offshore the Les Escoumins River is found at the toe of a submarine canyon but is unrelated to a deltaic body. This submarine canyon incises the margin of the Laurentian Channel and its source comprises exclusively the Les Escoumins River sediments since its head is confined between rocky headlands (Fig. 5C). Additionally, the head of the submarine canyon is located less than 1 km from the river mouth, providing a direct connection between river inflow and the submarine canyon. The high-resolution multibeam bathymetry imagery over this submarine canyon reveals the presence of crescentic bedforms related to the passage of relatively recent sediment density flows (Normandeau et al., 2015).

454 The base of the submarine fan is composed of the homogeneous mud of SU3 (Fig 6C).
455 Above SU3, seismic reflections are chaotic and suggest the presence of sediment
456 deposited by sediment density flows. The transition from SU3 to the chaotic seismic
457 reflections is estimated at 9-8.5 ka cal BP according to Duchesne et al. (2010).

458 Core 12PC (681 cm long), collected on the Les Escoumins River fan, is composed of 14
459 sediment density flow deposits (Fig. 8A). Most of these deposits are a few cm thick (≤ 10
460 cm) and characterized by a sharp increase in CT-numbers and magnetic susceptibility.
461 Grain-size properties indicate a fining-upward sequence with an erosive basal contact
462 (Fig. 8C). Mean grain-size generally reaches more than 200 µm. Two types of beds were
463 identified based on grading patterns: a first type characterized by a sharp increase
464 followed by a fining-upward sequence and a second type characterized by a thin (≤ 2 cm)
465 coarsening-upward sequence, followed by a thicker fining-upward sequence. Both types
466 are interpreted as a classical turbidite (Mulder and Alexander, 2001), where the basal
467 inverse grading is interpreted as the traction carpet associated with a prolonged shear
468 along the base of the flow (Sumner et al., 2008).

469 The thickest sediment density flow deposit within the core has a different
470 sedimentological signature. It consists of thick (> 1 m) homogeneous sand including mud
471 clasts (Fig. 8A). Its basal contact is sharp and erosional and no apparent grading pattern is
472 present in grain-size analysis. CT-numbers and magnetic susceptibility are generally high
473 among this facies except where mud clasts are present. This facies is interpreted as a
474 debris flow deposits resulting from a slope failure (Mulder and Alexander, 2001; Talling
475 et al., 2012).

476 The 14 sediment density flow deposits are distributed over the entire core, yet their
477 frequency and thickness decrease up-core. Organic matter collected at the base of core
478 12PC (670 cm) was dated 850 ± 65 cal BP (UCIAMS-127421) while shell fragments
479 collected at its top (117 cm) dated 540 ± 15 cal BP (UCIAMS-127440). These dates
480 suggest that sediment density flow deposits were frequent (5 in *ca.* 20 years) at the base
481 of the core, gradually becoming less frequent up-core (6 in *ca.* 300 years).

482 ***Longshore drift-fed submarine canyons/fans***

483 Nearby the Les Escoumins river-fed submarine fan, three additional submarine canyons
484 are located where the shelf narrows westward (Fig. 5C). These submarine canyons incise
485 the steep Laurentian Channel margin and are fed by longshore drift sediments (Gagné et
486 al., 2009; Normandeau et al., 2015). Unlike the submarine deltas described above, they
487 have no emerged component and have always been located below sea-level. The fan
488 bodies are *ca.* 25 m thick and are mainly observed in the top-half of the LSLE seismic
489 succession. They are mainly observed above SU3 and form lens-shaped and chaotic
490 features that downlap the underlying reflections. The reflections are generally chaotic and
491 disrupted over the fans while they are parallel and continuous on each side of them.
492 However, chaotic reflections, interpreted as mass movement deposits, are also observed
493 below the western fan, within the top half of SU3, while they are absent below the eastern
494 one. The eastern fan also appears to have formed later than the western one based on its
495 location in the seismic succession (Fig. 6D).

496 Core 13PC was collected on the eastern fan and is only 132 cm long (Fig. 8B). The size
497 and morphological expression of the fans, however, suggest that their evolution was

similar to the river-fed Les Escoumins fan (core 12PC) described in the previous section. Two sediment density flow deposits within core 13PC, interpreted as classical turbidites, are located at the same stratigraphic level as others in core 12PC. An age of 635 cal BP ± 20 (UCIAMS-127438) at 35 cm in core 13PC suggests a similar age for the two turbidites to those present in core 12PC (Fig. 8B).

DISCUSSION

Delta progradation and submarine fan deposition in a formerly glaciated region

The identification and dating of the different types of deposits observed at outcrop and in marine cores in the LSLE together with results from previous studies (Bernatchez, 2003; St-Onge et al., 2003; St-Onge et al., 2008; Duchesne et al., 2010), are used here to reconstruct the palaeogeographic context of delta progradation and submarine fan deposition in a deglaciation setting (Fig. 9). Based on stratigraphic architecture of the modern exposed component of the deltas, seismic stratigraphy and sediment core analysis, we build a simplified conceptual model of the approximate chronology for the transport of coarse terrigenous sediments to the LSLE since the late Wisconsinian (Fig. 9). The proposed model is divided into three major phases of delta progradation and submarine fan deposition. These three main phases overlap each other across the LSLE and no time boundaries are inferred. For instance, while the southern sector of the LSLE may pass into the second phase, the northern part may still be in the first phase. The first and/or second of these three phases may be absent in the evolution of some deltas of the LSLE, depending on the inherited local topography (width of the shelf, inland extent of drainage basin) and the pattern of ice margin retreat, as explained below. These three

520 phases are somewhat similar to Syvitski and Praeg (1989) sedimentation models but they
521 consider only submarine delta progradation and submarine fan formation instead of the
522 entire sedimentation of the LSLE.

523 ***Phase 1: Deltaic progradation on the shelf***

524 The first phase of deltaic evolution occurred during the retreat of the LIS margin and its
525 stabilization on the Québec North Shore around 12.5 ka cal BP (Shaw et al., 2002), when
526 RSL was ≥ 150 m higher than today (Dionne, 2001). On the shelf, the initial delta
527 progradation was marked by the rapid deposition of outwash fans directly at the
528 stabilized ice margin in a context of rapid RSL fall (up to 5 $cm.yr^{-1}$). The deposition of
529 outwash fans only spanned a few hundred years around 11 ka cal BP, according to
530 radiocarbon dates sampled in these deposits.

531 During this initial phase of delta progradation on the shelf, ice-proximal to ice-distal
532 glaciomarine sediments (SU2 and SU3) were deposited in the LSLE by meltwater
533 discharges (Fig. 9A; St-Onge et al., 2008; Duchesne et al., 2010). After the progressive
534 and spatially diachronous inland retreat of the LIS margin, glaciofluvial deltas fed by
535 sandy and silty glaciogenic materials began to prograde onto the LSLE shelf mainly by
536 accretion of beds deposited by sediment density flows, still in a context of RSL fall (Fig.
537 9A) (Bernatchez, 2003; Dietrich et al., 2016a).

538 This first stage is also characterized by mass movement processes (SU7) along the
539 steepest shores of the Laurentian Channel, as observed below the Les Escoumins fans
540 (Fig. 6D). These mass movements may have been responsible for initiating the submarine
541 canyons by retrogressive slope failures. Duchesne et al. (2010) also reported similar

chaotic reflections that they interpreted as mass movement deposits resulting from earthquakes in a rapidly uplifting margin due to crustal glacio-isostatic readjustment. These mass movements were probably triggered in response to the ongoing crustal readjustment following deglaciation (e.g., St-Onge et al., 2004). Following glacier retreat, maximum glacio-isostatic rebound generally leads to increased earthquake frequency (Johnson, 1989), which in turn likely generates mass movements along steep slopes, such as those observed in the LSLE (Pinet et al., 2015).

Phase 2: Laurentian Channel submarine fan deposition

The second phase of deltaic evolution and submarine fan deposition is characterized by the progradation of deltas into the Laurentian Channel (Fig. 9B). The delivery of sediments in the deeper waters of the LSLE was made possible by the deltaic progradation over the entire width of the shelf, and was thus achieved whenever deltaic progradation, which is dependent on sediment supply, lasted long enough to cover the entire width of the shelf. The depth of the shelf, constantly diminishing through time because of RSL fall, contributed in determining the extent of deltaic progradation. Thus, a narrow shelf and/or a long lasting glaciogenic sediment supply allowed sediments to be delivered into the Laurentian Channel. Conversely, a wide shelf and/or slow deltaic progradation did not permit the supply of deltaic material into the Laurentian Channel.

In the deep realm of the LSLE, the transition from SU3 to fan deposits is envisioned as recording the arrival of coarse-grained sediments delivered from the delta slope or river mouth in areas that were formerly dominated by the deposition of fine-grained sediment, its timing being controlled by the width of the shelf and spatial extent of deltaic

564 progradation. This transition occurred prior to 9-8.5 ka cal BP in the case of the
565 Manicouagan delta (SU3 to SU6; Duchesne et al., 2010) but no exact dates are available
566 for any of the deltas. River-derived sediment density flows and debris flows were the
567 main mechanisms of sediment transport through the submarine deltas. The presence of
568 debris flows suggests that they were produced by high sedimentation rates at river
569 mouths that increased the slope at the delta lip leading to frequent slope failures. Delta
570 channels would then have been used to evacuate these high-density flows. The debris
571 flows were also generated by seismic activity due to glacio-isostatic rebound. The late-
572 Wisconsinan / early-Holocene experienced increased earthquake frequency which likely
573 increased the frequency of debris flows at the delta fronts (Duchesne et al., 2003). The
574 increased earthquake frequency may also have increased landslides in the river
575 watershed, providing large volumes of sediment to rivers and their downstream deltas
576 (e.g., Dadson et al., 2004). Hyperpycnite-like deposits observed in cores from the
577 Manicouagan fans and in the Portneuf outcrops also indicate the occurrence of high
578 sediment concentration in the rivers during the early-Holocene that also favoured the
579 generation of river-derived density flows.

580 The accretion of the Manicouagan delta essentially continued until *ca.* 7 ka cal BP,
581 according to dates from the cores collected on the submarine fans. The main activity of
582 river-derived density flows ceased prior to 6970 ka cal BP in core 16PC (Fig. 7A). Cores
583 located farther away from the river mouth (17PC and 23PC) show that density flows
584 ceased as early as 9.5 ka cal BP, according to sedimentation rates derived from cores
585 16PC and 39PC. However, sediment density flow deposits identified in core 39PC from

586 the Manicouagan delta appear to have been deposited near 4 ka cal BP. It is difficult to
587 identify the exact type of deposits (slope failure vs river-derived deposits) in this core
588 because the sedimentary facies were deformed due to the coring process. These deposits
589 could represent exceptional flood events that allowed the formation of hyperpycnal flows.
590 Rather, due to their younger age, we suggest that they are turbidites since sediment
591 concentration in rivers was likely too low at *ca.* 4 ka cal BP to produce hyperpycnal
592 flows. Accumulation of sediments on the delta front and its failure is more likely at that
593 time. Since the Manicouagan system is considered as an end-member in terms of
594 sediment density flow activity, the other deltas in the LSLE are considered to have ceased
595 being active before 7 ka cal BP. For example, the activity of the Portneuf glaciofluvial
596 delta ceased well before that date, as exemplified by the construction of coastal suites at
597 10 ka cal BP. Additionally, the withdrawal of the LIS from its watershed occurred at *ca.*
598 10 ka cal BP, which corresponds to a drastic decrease in sediment supply at the river
599 mouth and the predominance of alongshore currents on sediment mobilization (Dietrich
600 et al., in press). In contrast, the withdrawal of the LIS from the Manicouagan watershed
601 occurred at *ca.* 7 ka cal BP, which corresponds to a decrease in meltwater-derived
602 sediment supply and in sediment density flow deposits on the Manicouagan submarine
603 fan.

604 Longshore transport was also active and remobilized deltaic and coastal sediments during
605 the progradation of the deltas into the Laurentian Channel. This transport of sediment
606 through longshore drift is suggested at that time for the onset of the western longshore
607 drift-fed fan in Les Escoumins, in combination with increased earthquake frequency

608 owing to crustal glacio-isostatic readjustment (Fig. 9B). Sediment supply from longshore
609 drift to the heads of the canyons on a narrow shelf and earthquakes would have generated
610 mass movements on the steep Laurentian Channel margin. The western fan appears to
611 have formed slightly earlier than the eastern one (Fig. 6D), probably in relation with a
612 slightly higher RSL; the coastal shelf being narrower at the head of the western canyon
613 than at that of the eastern one (Fig. 5C).

614 ***Phase 3: Delta erosion and longshore drift transport***

615 The third phase of submarine fan deposition is characterized by: 1) a drastic decrease in
616 submarine delta progradation; 2) the erosion of deltas on the shelf by coastal processes;
617 3) the deposition of coastal suites; and 4) the continuation of longshore drift transport to
618 the Les Escoumins canyons (Fig. 9C).

619 When the ice margin retreated from the river watersheds, sediment supply drastically
620 dropped while RSL fall rates decreased synchronously. In the Manicouagan region, the
621 LIS left the watershed at *ca.* 7 ka cal BP (Fig. 2). Therefore, the Manicouagan delta could
622 no longer produce river-derived density flows or other sediment density flows due to the
623 reduced sediment supply; instead, it experienced coastal erosion where sediments were
624 remobilized and transported through longshore drift (e.g., Bernatchez, 2003). In the
625 Portneuf region, the LIS left the watershed by *ca.* 10 ka cal BP which induced as well a
626 decrease in sediment density flow activity. Here, sediments were eroded at the delta front
627 and were remobilized and transported to adjacent bays or to areas where the coastal shelf
628 is wider, while RSL was still falling. In the Portneuf region, most of the sediment
629 accumulated in raised spit complexes downdrift of the former glaciofluvial delta (Fig. 4I)

630 and in the adjacent bay to the south-west (Fig. 5A). The deposition of nearshore sand
631 sheets and spit platforms occurred after the demise of the glaciofluvial delta progradation,
632 as indicated by the erosion and reworking of these deltas by shore-related processes
633 (waves and longshore-drift; Fig. 4A). The material involved within these coastal suites
634 derived almost exclusively from the delta itself. Since in distinct delta systems the shore-
635 related structures are found below different altitudes depending on the studied deltaic
636 succession, an allogenic process such as an increase of the wave regime in the LSLE is
637 unlikely. A local forcing is rather proposed to explain the diachronic onset of the
638 development of the shore-related structures over delta systems of the LSLE. The retreat
639 of the ice margin from the drainage basins of feeder rivers is interpreted as having
640 permitted the development of shore-related structures by an abrupt decrease of the fluvial
641 sediment supply / wave energy ratio (e.g., Swenson et al., 2005). At the scale of the
642 LSLE, the onset of the development of shore-related structures was necessarily
643 diachronic and depended on the pattern of retreat of the continental ice margin (Occhietti
644 et al., 2011) and the northern extent of drainage basins (Fig. 2). The deposition of the
645 shore-related structures does not relate to the deltaic progradation but rather to a
646 redistribution of formerly-deposited glaciofluvial sediments. The timing of the transition
647 from a deltaic progradation, either restricted to the shelf (phase 1), or having reached the
648 Laurentian Channel (phase 2) to the erosion of the delta and the generalization of
649 longshore-drift transport (phase 3) is then solely controlled by the inland extent of the
650 drainage basin and the pattern of ice margin retreat. A restricted drainage basin and/or a
651 rapid retreat of the ice margin over the drainage basin permitted an early transition to

652 phase 3, as it was the case for the Portneuf delta (Fig. 2). To the opposite, extensive
653 drainage basin permitted a long lasting deltaic progradation and a late transition to phase
654 3 (example of the Manicouagan delta, Fig. 2), even though the RSL curve was similar
655 throughout the LSLE.

656 Part of the sediment from the Portneuf region, between Les Escoumins and the Portneuf
657 delta, is believed to have been transported to the heads of the Les Escoumins canyons,
658 allowing the eastern fan of the Les Escoumins system to form and develop (Fig. 6D).
659 Coastal erosion on delta fronts would have been amplified during the early-Holocene due
660 to the decrease of sediment supply from rivers, in a similar pattern as what was observed
661 on the Moisie Delta (Dubois, 1979; Normandeau et al., 2013). This increased erosion at
662 the delta fronts allowed an increase in sediment transport towards the longshore drift-fed
663 canyons which in turn allowed them to remain active throughout the Holocene.

664 The river-fed Les Escoumins fan also continued its activity during the mid- to late-
665 Holocene, as opposed to the other deltas in the LSLE. In this case, the river-fed Les
666 Escoumins canyon is directly connected to the river and is located on a steep slope. Two
667 hypotheses are invoked to explain the activity of the Les Escoumins canyon and the
668 occurrence of debris flow deposits and turbidites: (a) sediment supply to the heads of the
669 canyons and/or (b) earthquake-induced shaking. Earthquakes could have played a role in
670 triggering mass movements since the Les Escoumins canyons are located *ca.* 100 km east
671 from the Charlevoix-Kamouraska seismic zone (CKSZ), the most active seismic zone in
672 Eastern Canada (Lamontagne, 1987). However, earthquakes were more frequent prior to
673 4 ka BP with recurrence rates of 300 years (St-Onge et al., 2004) and cannot explain the

14 turbidites and debrites observed in core 12PC that were deposited during the last 1000 years. Therefore, sediment supply to the Les Escoumins sector must have played a role in triggering them. Down-canyon remobilization was favoured in these sectors due to sediment supply from the Les Escoumins River (although diminished by the early-Holocene) and the erosion of the neighbouring shorelines. Wetter periods could have increased sediment supply to the river mouth, as suggested by the ages of sediment density flow activity obtained for the Les Escoumins canyons, which are also consistent with the warm and humid medieval period (Mann et al., 1999). The steep slopes present directly at the river mouth could then have favoured the generation of slope failures. The increase in sediment supply would not have been high enough to generate river-derived density flows on the other river-fed delta systems which have lower slopes and broader shelves (Normandeau et al., 2015).

Controls on the activity and location of submarine fans on a formerly glaciated coast and shelf

The delivery of coarse sediment to the LSLE continued throughout the Holocene and since the early stages of deglaciation. Three main controls are identified as playing a role in contributing to the continuation in coarse sediment delivery: 1) type (glaciofluvial, fluvial or longshore drift), rate and duration of sediment supply; 2) geomorphology of the shelf; and 3) RSL. While the type, rates and duration of sediment supply controlled the chronology of deposition and RSL controlled the location of deposition, the morphology of the shelf controlled both.

695 The type,rate and duration of sediment supply, which is mostly controlled by the style of
696 deglaciation and the drainage basin (watershed area), was the primary control over
697 sediment delivery in the LSLE. During the early stages of deglaciation, outwash fans
698 formed at the edge of the Laurentian Highlands (Dietrich et al., 2016a). The sediments
699 were directly delivered from a nearby glacial source, and consist, in the proximal domain
700 i.e., on the inner coastal shelf, of very-coarse-grained deposits (gravel and boulders)
701 emplaced through subglacial flow deconfinement processes (e.g., Russell and Arnott,
702 2003). However, in more distal settings but still on the coastal shelf, deposition of sand
703 and silt by sediment density flows dominated. As soon as the ice margin retreated inland,
704 the type of sediment supply changed from a direct ice-contact source to a glaciofluvial
705 one. There was a fundamental difference in terms of type of sediment deposited at the
706 coast: while the ice-contact source provided gravel and boulders to outwash fans, the
707 glaciofluvial source essentially provided sand- and silt-sized sediments, allowing large
708 deltas to form in the LSLE. Since glacial ice was still in the river watersheds, the deltas
709 grew in volume and area and, in some cases, reached the edge of the Laurentian Channel
710 (transition from Phase 1 to Phase 2, Fig. 9). Sediment supply from the rivers drastically
711 reduced when the ice margin left the watersheds of the rivers, driving the transition from
712 a fluvially-dominated Phase 1 or 2 to a wave-dominated Phase 3 (Fig. 9). The decrease in
713 sediment supply from the rivers did not occur simultaneously in all the rivers since their
714 watershed vary greatly in extent. The smaller watersheds were abandoned far before the
715 larger ones, which explains why the Manicouagan delta is an end-member for the activity
716 of sediment density flow due to its large size. The ice margin left the Manicouagan

watershed by *ca.* 7 ka cal BP, which is consistent with a reduced sediment density flow activity near 7 ka cal BP observed in the cores. In contrast, the ice margin left the Portneuf watershed as early as *ca.* 10 ka cal BP, which explains why the channels observed offshore the river are buried and why coastal suites formed near 10 ka cal BP.

While deltas were highly constructive during the early stages of deglaciation, they began to be highly eroded following the retreat of the ice margin from the watersheds. The erosion of the delta fronts began while RSL fall rates had reduced or were close to stabilization. The erosion of the delta fronts then led to a change in the delivery of coarse sediment to the Laurentian Channel. In deltaic settings, coarse sediment delivery ceased because their fronts were eroded and the sediment was transported to adjacent bays. Additionally, the reduced rates of sediment supply due to the retreat of the ice-margin from the watersheds reduced sediment concentration in the rivers, thereby preventing the generation of river-derived density flows at the delta fronts.

Shelf geomorphology had a major influence on the sediment delivery to the Laurentian Channel. The shelf width controlled the transition from Phase 1 to Phase 2 as well as the continued sediment density flow activity in submarine canyons. For example, in the Les Escoumins river-fed fan, the shelf geomorphology allowed a continuation in coarse sediment delivery to the Laurentian Channel during postglacial times. This continuation in coarse sediment delivery was possible because the steep slopes favoured failure at the canyon head, as evidenced by the presence of turbidites instead of hyperpycnite-like deposits. Therefore, both the Les Escoumins river-fed and longshore drift-fed systems continued delivering sediment due to the narrow shelf that allowed a direct connection

739 between a source of sediment supply and a steep slope. Conversely, the wide shelf in
740 front of the major deltas of the North Shore (e.g., Portneuf) prevented a direct connection
741 with the steep slopes of the Laurentian Channel, which in turn prevented locally the
742 development of a Phase 2 in these areas.

743 In this formerly-glaciated marine basin, RSL did not play a major role in delivering
744 coarse sediment to the LSLE. In fact, RSL only controlled the location of the delivery of
745 coarse sediment. This finding contrasts with a previous study by Hart and Long (1996)
746 that stated that RSL fluctuations was the primary driver on sediment delivery. Indeed,
747 sediment delivery occurred during RSL fall but, as exemplified by the Portneuf delta, it
748 did not lead to increased sediment delivery. During the early stages of deglaciation,
749 coarse sediment accumulated mostly on the wide shelf due to a high RSL. Sediment was
750 rapidly delivered to the deeper Laurentian Channel as the RSL was rapidly falling.
751 Sediments were no longer being transferred to the Laurentian Channel via river-fed
752 channels even though RSL was still falling when the ice margin left the watersheds.
753 Unlike sequence stratigraphic models predict, the falling stages or lowstands of RSL did
754 not favour sediment density flow activity in the Laurentian Channel, despite the transition
755 to deep-water systems developing steeper depositional slopes, because sediment supply
756 had diminished. Therefore, RSL did not play a key role in the chronology of the sediment
757 transport. In combination with the shelf morphology (narrow vs. wide), it however
758 controlled the location of sediment deposition either on the shelf or in the Laurentian
759 Channel.

760 **Comparison with non-glaciated margins**

761 Covault and Graham (2010) summarized four main types of settings that lead to different
762 timings in sediment delivery to marine basins: 1) fluvially-fed canyons that incise
763 continental shelves to the shoreline that can exhibit continuous sediment deposition,
764 regardless of RSL; 2) longshore drift-fed canyons that can be active only during
765 highstands because of sediment by-passing along the shores; 3) fluvially-fed canyons
766 located away from the shoreline that can be active during RSL highstands if sediment
767 supply allows the deltas to prograde onto the broad shelf (e.g., Burgess and Hovius,
768 1998); and 4) fluvially-fed systems that are located on broad shelves that can be active
769 only during sea-level lowstands, when there is a direct connection between river mouths
770 and submarine canyons.

771 The interaction between the different types of submarine canyons/channels along a same
772 margin are poorly documented, except along the California borderland (Covault et al.,
773 2007; Normark et al., 2009; Romans et al., 2009; Covault and Graham, 2010) and along
774 the Chilean margin (Bernhardt et al., 2016). In this respect, the analysis of the activity of
775 the submarine fans along the LSLE brings new insights into the dynamics of sediment
776 transport in a geological setting characterized by deglaciation, a rapid change in type and
777 rates of sediment supply and a varying shelf geomorphology.

778 The modification of terrigenous supply to the Laurentian Channel has some similar
779 characteristics with the deep-water turbidite systems bordering the Californian Coast
780 (Covault et al., 2007; Normark et al., 2009; Romans et al., 2009; Covault and Graham,
781 2010). In the California borderland systems, canyons supplied by fluvial sediments were
782 mainly active during sea-level lowstands while canyons supplied by longshore drift were

draped by hemipelagic sediments. This difference in activity was due to a direct connection between the river mouths and the canyons which limited longshore drift towards longshore drift-fed canyons. Following the Holocene eustatic transgression, the disconnection of the canyon heads from fluvial input led to the formation of the large Oceanside littoral cell which allowed the transport of sediments to the longshore drift-fed canyon of La Jolla (Covault et al., 2007). In the LSLE, the modification in sediment delivery occurred during a forced regression. According to the conceptual model of Covault and Graham (2010) for the California borderland, it should be expected that sediment supply changes from longshore drift to fluvial in this regression context since lowstand intervals favour a direct connection between rivers and submarine channels. The opposite was observed in the LSLE where the activity of the river-fed channels in the LSLE was drastically reduced while the longshore drift-fed canyons continued to be active (Fig. 9). This modification of terrigenous supply is partly due to the different tectonic settings, where the California active margin favours the formation of canyons while the LSLE margin favours the formation of submarine deltas on which channels form. However, the key control in the LSLE is the ice-margin position within the watersheds that controlled sediment supply to the rivers, whereas the shelf width is the key control over sediment delivery on the California borderland (Covault et al., 2007).

Moreover, terrigenous sediment supply is not constant in the LSLE and is not primarily controlled by RSL fluctuations. RSL rather defined the base level at which the deltas or fans were formed. When RSL fell to its present level, sediment density flows reached the Laurentian Channel while during the Goldthwait Sea (highstand), sediment density flows

805 were depositing coarse sediment on the coastal shelf. Terrigenous sediment supply is
806 more influenced by the presence of a glacier in the watershed (Dietrich et al., in press) or
807 paragacial conditions where rivers supply important amounts of sediment to the sea.
808 Sediment supply was greater during the late-Wisconsinan due to the presence of the LIS
809 margin which supplied large volumes of sediment capable of forming large submarine
810 deltas (Fig. 9). The RSL fall then allowed deltas to evolve on the coastal shelf and
811 eventually into the Laurentian Channel, although it did not control the formation of
812 sediment density flows.

813 These observations are thus in agreement with Covault and Graham (2010) and
814 Evangelinos et al. (in press) that suggested that high-latitude turbidite systems are mainly
815 controlled by glacial sediment supply rather than RSL fluctuations. These results also
816 support statements from Knudson and Hendy (2009) and Covault et al. (2007) that
817 demonstrated that submarine fans with similar climatic conditions and located in close
818 proximity with each other can have different rates of activity and different sedimentary
819 processes, depending on their source of sediment and their geomorphological setting.

820 **CONCLUSIONS**

821 This study, based on the integration of terrestrial and marine datasets, demonstrates that
822 submarine fan deposition in the LSLE since deglaciation is divided into three phases: 1) a
823 first phase marked by the deposition of outwash fans and delta progradation on the shelf
824 during the retreat of the LIS margin; 2) a second phase marked by high glaciofluvial
825 sediment supply from rivers, which led to the triggering of debris flows and river-derived
826 sediment density flows and the formation of large submarine deltas into the Laurentian

827 Channel; and 3) a third phase marked by a reduced sediment supply from rivers which
828 favoured coastal erosion along the delta fronts and the transfer of sediments to canyon
829 heads by longshore drift, where the shelf narrows.

830 The delivery of coarse sediment to marine basins is often viewed as essentially controlled
831 by RSL variations. In a formerly glaciated margin, RSL variations have little effect on
832 sediment delivery compared to the type, rate and duration of sediment supply and shelf
833 geomorphology. The presence of glacial ice in river watersheds largely controls the
834 volume of sediment supplied to marine basins. Therefore, during sea-level highstands and
835 regressions, coarse sediments can be delivered to marine basins due to increased
836 sediment supply from the glacially-fed rivers. During lowstands, when sediment transport
837 is supposed to be active according to sequence stratigraphic models, the absence of
838 glacial ice in the watersheds reduces drastically the amount of sediment supplied to the
839 marine basin. Therefore, deltas change from river-dominated to wave-dominated and
840 become largely eroded. Sediments are then transported through longshore drift in
841 adjacent bays or to areas where the shelf narrows. In these narrow shelves, sediments are
842 delivered to deeper marine basin because of the direct connection between longshore
843 sediment supply and a steep slope.

844 Sediment dynamics in high-latitude environments such as the LSLE thus differ from
845 lower latitudes deltaic and canyon systems because they were previously glaciated and do
846 not respond to the same forcing mechanisms as others, namely RSL. This paper
847 highlights the role of the type of sediment supply (ice-contact, glacio-fluvial and
848 longshore drift) in the timing and activity of submarine fans in high-latitude

environments. It also highlights how structural inheritance, which controls the watershed area and the shelf geomorphology, is more important than RSL fluctuations in maintaining deltaic activity in formerly glaciated environments.

ACKNOWLEDGEMENTS

AN and PD contributed equally to the writing of this manuscript. We sincerely thank the captain, crew, and scientific participants of the COR0602, COR1002, COR1203 cruises on board the R/V Coriolis II and the LEH1201 on the R/V Louis-Edmond-Hamelin. We also thank the *Canadian Hydrographic Service* for providing multibeam echosounder datasets. François Lapointe (INRS) is thanked for help in thin section preparation. This study was supported by the Natural Sciences and Engineering Research Council of Canada through Discovery and Ship-time grants to P.L., G.S. and Jacques Locat (Université Laval), by the Fond de Recherche Québécois – Nature et Technologie scholarship to A.N. and by the Canadian Foundation for Innovation and the Ministère de l'éducation du Québec through equipment grants to P.L. P. Dietrich and J.-F. Ghienne are grateful to the action SYSTER program of the INSU-CNRS (Institut National des Sciences de l'Univers, Centre National de la Recherche Scientifique) that founded field campaigns. This work is a contribution to the "SeqStrat-Ice" ANR project 12-BS06-14. Finally, we thank David Piper for his comments on a previous version of this manuscript as well as associate editor Jeffrey Clark, Jean Roger and an anonymous reviewer for their comments that improved the quality of this paper.

869 **REFERENCES CITED**

870 Babonneau, N., Delacourt, C., Cancouët, R., Sisavath, E., Bachèlery, P., Mazuel, A.,
871 Jorry, S.J., Deschamps, A., Ammann, J., and Villeneuve, N., 2014, Direct sediment
872 transfer from land to deep-sea: Insights into shallow multibeam bathymetry at La
873 Réunion Island: Marine Geology , v. 346, p. 47-57.

874 Bernatchez, P., 2003, Évolution littorale holocène et actuelle des complexes deltaïques de
875 Betsiamites et de Manicouagan-Outardes: Synthèse, processus, causes et
876 perspectives [Ph.D. thesis]: Québec, Université Laval, 531 p.

877 Bernatchez, P., and Dubois, J.-M.M., 2004, Bilan des connaissances de la dynamique de
878 l'érosion des côtes du Québec maritime laurentien: Géographie physique et
879 Quaternaire, v. 58, p. 45-71.

880 Bernhardt, A., Hebbeln, D., Regenberg, M., Lückge, A., and Strecker, M.R., 2016,
881 Shelfal sediment transport by an undercurrent forces turbidity-current activity during
882 high sea level along the Chile continental margin: Geology, v. 44, p.295-298.

883 Blott, S.J., and Pye, K., 2001, GRADISTAT: a grain size distribution and statistics
884 package for the analysis of unconsolidated sediments: Earth Surface Processes and
885 Landforms, v. 26, p. 1237-1248.

886 Boulton, G.S., 1990, Sedimentary and sea level changes during glacial cycles and their
887 control on glacimarine facies architecture, *in* Dowdeswell, J.A., and Scourse, J.D.,

888 eds., Glacimarine Environments: Processes and sediments: Geological Society
889 [London] Special Publication 53, p. 15-52.

890 Bouma, A.H., 1962, Sedimentology of some flysch deposits: A graphic approach to
891 facies interpretation: Amsterdam, Elsevier, 168 p.

892 Bouma, A.H., 2004, Key controls on the characteristics of turbidite systems, *in* Lomas,
893 S.A., and Joseph, P., eds., Confined Turbidite Systems: Geological Society [London]
894 Special Publication 222, p. 9-22.

895 Boyd, R., Ruming, K., Goodwin, I., Sandstrom, M., and Schröder-Adams, C., 2008,
896 Highstand transport of coastal sand to the deep ocean: A case study from Fraser
897 Island, southeast Australia: Geology, v. 36, p. 15-18.

898 Burgess, P.M., and Hovius, N., 1998, Rates of delta progradation during highstands:
899 consequences for timing of deposition in deep-marine systems: Journal of the
900 Geological Society [London], v. 155, p. 217-222.

901 Clare, M.A., Hughes Clarke, J.E., Talling, P.J., Cartigny, M.J.B., and Pratomo, D.G.,
902 2016. Preconditioning and triggering of offshore slope failures and turbidity currents
903 revealed by most detailed monitoring yet at a fjord-head delta. Earth and Planetary
904 Science Letters, v. 450, p. 208-220.

905 Conway, K.W., Barrie, J.V., Picard, K., and Bornhold, B.D., 2012, Submarine channel
906 evolution: active channels in fjords, British Columbia, Canada: Geo-Marine Letters,
907 v. 32, p. 301-312.

908 Corner, G.D., 2006, A transgressive-regressive model of fjord-valley fill: stratigraphy,
909 facies and depositional controls: SEPM Special Publication, v. 85, p. 161-178.

910 Covault, J.A., and Graham, S.A., 2010, Submarine fans at all sea-level stands: Tectono-
911 morphologic and climatic controls on terrigenous sediment delivery to the deep sea:
912 Geology, v. 38, p. 939-942.

913 Covault, J.A., Normark, W.R., Romans, B.W., and Graham, S.A., 2007, Highstand fans
914 in the California borderland: The overlooked deep-water depositional systems:
915 Geology, v. 35, p. 783.

916 Dadson, S.J., Hovius, N., Chen, H., Dade, W.B., Lin, J.-C., Hsu, M.-L., Lin, C.-W.,
917 Horng, M.-J., Chen, T.-C., Milliman, J., and Stark, C.P., 2004. Eartquake-triggered
918 increase in sediment delivery from an active moutain belt: geology, v. 32, p. 733-
919 736.

920 Dietrich, P., 2015, Faciès, architectures stratigraphiques et dynamiques sédimentaires en
921 contexte de régression forcée glacio-isostatique, École doctorale des sciences de la
922 terre et de l'environnement [Ph.D. thesis]: Strasbourg, Université de Strasbourg, 410
923 p.

924 Dietrich, P., Ghienne, J.-F., Normandeau, A., and Lajeunesse, P., 2016a, Upslope –
925 migrating bedforms in a proglacial sandur delta : cyclic steps from river-derived
926 underflows?: Journal of Sedimentary Research, v. 86, p. 113-123.

927 Dietrich, P., Ghienne, J.F., Schuster, M., Lajeunesse, P., Nutz, A., Deschamps, R.,
928 Rosuin, C., and Duringer, P., From outwash to coastal systems in the Portneuf-
929 Forestville deltaic complex (Québec North Shore): the drainage basin as lead actor in
930 forced-regressive, deglacial sequences: Sedimentology, (in press), doi:
931 10.1111/sed.12340.

932 Dionne, J.C., 2001, Relative sea-level changes in the St. Lawrence estuary from
933 deglaciation to present day: Geological Society of America Special Paper 351, p.
934 271-284.

935 Dubois, J.-M., 1979, Environnement quaternaire et évolution post-glaciaire d'une zone
936 côtière en émersion en bordure sud du Bouclier Canadien: la Moyenne Côte-Nord du
937 Saint-Laurent, Québec [Ph.D. thesis], Ottawa, Université d'Ottawa, 794 p.

938 Ducassou, E., Migeon, S.B., Mulder, T., Murat, A., Capotondi, L., Bernasconi, S.M., and
939 Mascle, J., 2009, Evolution of the Nile deep-sea turbidite system during the Late
940 Quaternary: influence of climate change on fan sedimentation: Sedimentology, v. 56,
941 p. 2061-2090.

942 Duchesne, M.J., Long, B.F., Urgeles, R., Locat, J., 2002, New evidence of slope
943 instability in the Outardes Bay delta area, Quebec, Canada: Geo-Marine Letters, v.
944 22, p. 233-242.

945 Duchesne, M.J., 2005, Apport de méthodes géophysiques marines et de la scanographie à
946 l'étude de la genèse des faciès de sismique-réflexion de haute et de très haute
947 résolution [Ph.D. thesis], Québec, INRS-ETE, 440 p.

948 Duchesne, M.J., Pinet, N., Bédard, K., St-Onge, G., Lajeunesse, P., Campbell, D.C., and
949 Bolduc, A., 2010, Role of the bedrock topography in the Quaternary filling of a giant
950 estuarine basin: the Lower St. Lawrence Estuary, Eastern Canada: Basin Research, v.
951 22, p. 933-951.

952 Eilertsen, R.S., Corner, G.D., Assheim, O., and Hansen, L., 2011, Facies characteristics
953 and architecture related to palaeodepth of Holocene fjord-delta sediments:
954 Sedimentology, v 58, p. 1784-1809.

955 Evangelinos, D., Nelson, C.H., Escutia, C., De Batist, M., and Khlystov, O., in press.
956 Late-Quaternary climatic control of Lake Baikal (Russia) turbidite systems:
957 Implications for turbidite systems worldwide: Geology.

958 Fortin, D., Francus, P., Gebhardt, A.C., Hahn, A., Kliem, P., Lisé-Pronovost, A.,
959 Roychowdhury, R., Labrie, J., and St-Onge, G., 2013, Destructive and non-
960 destructive density determination: method comparison and evaluation from the
961 Laguna Potrok Aike sedimentary record: Quaternary Science Reviews, v. 71, p. 147-
962 153.

963 Francus, P., 1998, An image-analysis technique to measure grain-size variation in thin
964 sections of soft clastic sediments: Sedimentary Geology, v. 121, p. 289-298.

965 Francus, P., and Nobert, P., 2007, An integrated computer system to acquire, measure,
966 process and store image of laminated sediments: International limnogeology
967 congress, 4th, Barcelona, Abstract.

968 Gagné, H., Lajeunesse, P., St-Onge, G., and Bolduc, A., 2009, Recent transfer of coastal
969 sediments to the Laurentian Channel, Lower St. Lawrence Estuary (Eastern Canada),
970 through submarine canyon and fan systems: Geo-Marine Letters, v. 29, p. 191-200.

971 Hart, B.S. and Long, B.F., 1996, Forced regressions and lowstand deltas: Holocene
972 canadian examples: Journal of Sedimentary Research, v. 66, p. 820-829.

973 Hill, P.R., 2012, Changes in submarine channel morphology and slope sedimentation
974 patterns from repeat multibeam surveys in the Fraser River delta, western Canada, *in*
975 Li, M.Z., Sherwood, C.R., and Hill, P.R., eds., Sediments, Morphology and
976 Sedimentary Processes on Continental Shelves: International Association of
977 Sedimentologists, Special Publication 44, p. 47-70.

978 Hughes Clarke, J., Vidiera Marques, C.R., and Pratomo, D., 2014, Imaging Active Mass-
979 Wasting and Sediment Flows on a Fjord Delta, Squamish, British Columbia, *in*
980 Krastel, S., Behrmann, J.-H., Völker, D., Stipp, M., Berndt, C., Urgeles, R., Chaytor,
981 J., Huhn, K., Strasser, M., and Harbitz, C.B., eds., Submarine Mass Movements and
982 Their Consequences, Advances in Natural and Technological Hazards Research 37,
983 Springer, p. 249-260.

Jeagle, M., 2014, Nature et origine des sédiments de surface de l'estuaire du Saint-Laurent [M.Sc. thesis]: Rimouski, ISMER-UQAR, 79 p.

Johnston, A.C., 1989, The effect of large ice sheets on earthquake genesis. *in* Gregersen,S., and Basham, P.W., (eds) Earthquakes at North Atlantic Passive Margins: Neotectonics and Postglacial Rebound, p. 581-599. Kluwer Academic Publishers, Dordrecht 1989.

Josenhans, H., and Lehman, S., 1999, Late glacial stratigraphy and history of the Gulf of St. Lawrence, Canada: Canadian Journal of Earth Sciences, v. 36, p. 1327-1345.

Khripounoff, A., Vangriesheim, A., Crassous, P., and Etoubleau, J., 2009, High frequency of sediment gravity flow events in the Var submarine canyon (Mediterranean Sea): Marine Geology, v. 263, p. 1-6.

Knudson, K.P., and Hendy, I.L., 2009, Climatic influences on sediment deposition and turbidite frequency in the Nitinat Fan, British Columbia: Marine Geology, v. 262, p. 29-38.

Lajeunesse, P., 2016, Late-Quaternary grounding-zone wedges, NW Gulf of St. Lawrence, Eastern Canada, *in* Dowdeswell, J., Canals, M., Jakobsson, M., Todd, B., Dowdeswell, E., and Haan, K., Atlas of Submarine Glacial Landforms: Modern, Quaternary and Ancient: Geological Society [London] Memoir Paper 897, (in press), doi:.

1003 Lamb, M.P., and Mohrig, D., 2009, Do hyperpycnal-flow deposits record river-flood
1004 dynamics?: Geology, v. 37, p. 1067-1070.

1005 Lamontagne, M., 1987, Seismic activity and structural features in the Charlevoix region,
1006 Quebec: Canadian Journal of Earth Sciences, v. 24, p. 2118-2129.

1007 Lewis, K.B., and Barnes, P.M., 1999, Kaikoura Canyon, New Zealand: active conduit
1008 from near-shore sediment zones to trench-axis channel: Marine Geology, v. 162, p.
1009 39-69.

1010 Mann, M.E., Bradley, R.S., and Hughes, M.K., 1999, Northern Hemisphere
1011 Temperetaures During the Past Milleniums: Inferences, Uncertainties, and
1012 Limitations: Geophysical Research Letters, v. 26, p. 759-762.

1013 Marchand, J.-P., Buffin-Bélanger, T., Hétu, B. and St-Onge, G., 2014. Stratigraphy and
1014 infill history of the glacially eroded Matane River Valley, eastern Quebec,
1015 Canada: Canadian Journal of Earth Sciences, v. 51, p. 105–124.

1016 Marshall, S.J., Tarasov, L., Clarke, G.K.C., and Peltier, W.R., 2000, Glaciological
1017 reconstruction of the Lauentide Ice Sheet: physical processes and modelling
1018 challenges: Canadian Journal of Earth Sciences, v. 37, p. 769-793.

1019 Maslin, M., Knutz, P.C., and Ramsay, T., 2006, Millennial-scale sea-level control on
1020 avulsion events on the Amazon Fan: Quaternary Science Reviews, v. 25, p. 3338-
1021 3345.

1022 Migeon, S., Mulder, T., Savoye, B., and Sage, F., 2006, The Var turbidite system
1023 (Ligurian Sea, northwestern Mediterranean)—morphology, sediment supply,
1024 construction of turbidite levee and sediment waves: implications for hydrocarbon
1025 reservoirs: Geo-Marine Letters, v. 26, p. 361-371.

1026 Mulder, T., and Alexander, J., 2001, The physical character of subaqeous sedimentary
1027 density flows and their deposits: Sedimentology, v. 48, p. 269-299.

1028 Mulder, T., Syvitski, J.P.M., Migeon, S., Faugères, J.-C., and Savoye, B., 2003, Marine
1029 hyperpycnal flows: initiation, behavior and related deposits. A review: Marine and
1030 Petroleum Geology, v. 20, p. 861-882.

1031 Normandeau, A., Lajeunesse, P., and St-Onge, G., 2013, Shallow-water longshore drift-
1032 fed submarine fan deposition (Moisie River Delta, Eastern Canada): Geo-Marine
1033 Letters, v. 33, p. 391-403.

1034 Normandeau, A., Lajeunesse, P., and St-Onge, G., 2015, Submarine canyons and
1035 channels in the Lower St. Lawrence Estuary (Eastern Canada): Morphology,
1036 classification and recent sediment dynamics: Geomorphology, v. 241, p. 1-18.

1037 Normandeau, A., Lajeunesse, P., St-Onge, G., Bourgault, D., St-Onge Drouin, S.,
1038 Senneville, S., and Bélanger, S., 2014, Morphodynamics in sediment-starved inner-
1039 shelf submarine canyons (Lower St. Lawrence Estuary, Eastern Canada): Marine
1040 Geology, v. 357, p. 243-255.

1041 Normark, W.R., Piper, D.J.W., Romans, B.W., Covault, J.A., Dartnell, P., and Sliter,
1042 R.W., 2009, Submarine canyon and fan systems of the California Continental
1043 Borderland: The Geological Society of America Special Paper 454, p. 141-168.

1044 Nutz, A., Ghienne, J.-F., Schuster, M., Dietrich, P., Roquin, C., Hay, M.B., Bouchette, F.,
1045 and Cousineau, P.A., 2015, Forced regressive deposits of a deglaciation sequence:
1046 example from the Late Quaternary succession in the Lake Saint-Jean basin (Québec,
1047 Canada): Sedimentology, v. 62, p. 1593-1610.

1048 Occhietti, S., Parent, M., Lajeunesse, P., Robert, F., and Govare, É., 2011, Late
1049 Pleistocene–Early Holocene Decay of the Laurentide Ice Sheet in Québec–Labrador,
1050 *in* Ehlers, J., Gibbard, P.L., Hughes, P.D., eds, Quaternary glaciations - Extent and
1051 chronology: Development in Quaternary Science 15, p. 601-630.

1052 Paull, C.K., McGann, M., Sumner, E.J., Barnes, P.M., Lundsten, E.M., Anderson, K.,
1053 Gwiazda, R., Edwards, B., and Caress, D.W., 2014, Sub-decadal turbidite frequency
1054 during the early Holocene: Eel Fan, offshore northern California: Geology, v. 42, p.
1055 855-858.

1056 Peltier, W.R., Argus, D.F., and Drummond, R., 2015, Space geodesy constrains ice age
1057 terminal deglaciation: The global ICE-6G_C (VM5a) model: Journal of Geophysical
1058 Research: Solid Earth, v. 120, p. 450-487.

1059 Pinet, N., Brake, V., Campbell, D.C., and Duchesne, M.J., 2011, Seafloor and Shallow
1060 Subsurface of the St. Lawrence River Estuary: Geoscience Canada, v. 38, p. 31-40.

1061 Postma, G., Cartigny, M., and Kleverlaan, K., 2009, Structureless, coarse-tail graded
1062 Bouma Ta formed by internal hydraulic jump of the turbidity current?: Sedimentary
1063 Geology, v. 219, p. 1-6.

1064 Porębski, S.J., and Steel, R.J., 2003, Shelf-margin deltas: their stratigraphic significance
1065 and relation to deep-water sands: Earth-Science Reviews, v. 62, p. 283-326.

1066 Prior, D.B., and Bornhold, B.D., 1989, Submarine sedimentation on a developing
1067 Holocene fan delta: Sedimentology, v. 36, p. 1053-1076.

1068 Reimer, P.J., Bard, E., Bayliss, A., Beck, J.W., Blackwell, P.G., Ramsey, C.B., Buck,
1069 C.E., Cheng, H., Edwards, R.L., Friedrich, M., Grootes, P.M., Guilderson, T.P.,
1070 Haflidason, H., Hadjas, I., Hatté, C., Heaton, T.J., Hoffman, D.L., Hogg, A.G.,
1071 Hughen, K.A., Kaiser, K.F., Kromer, B., Manning, S.W., Niu, M., Reimer, R.W.,
1072 Richards, D.A., Scott, E.M., Southon, J.R., Staff, R.A., Turney, C.S.M., and van der
1073 Plicht, J., 2013, Intcal13 and Marine13 radiocarbon age calibration curves 0-50,000
1074 years cal BP: Radiocarbon, v. 55, p. 1869-1887.

1075 Roger, J., Saint-Ange, F., Lajeunesse, P., Duchesne, M.J., and St-Onge, G., 2013, Late
1076 Quaternary glacial history and meltwater discharges along the Northeastern
1077 Newfoundland Shelf: Canadian Journal of Earth Sciences, v. 50, p. 1178-1194.

1078 Rogers, K.G., and Goodbred, S.L., 2010, Mass failures associated with the passage of a
1079 large tropical cyclone over the Swatch of No Ground submarine canyon (Bay of
1080 Bengal): Geology, v. 38, p. 1051-1054.

1081 Romans, B.W., Normark, W.R., McGann, M.M., Covault, J.A., and Graham, S.A., 2009,
1082 Coarse-grained sediment delivery and distribution in the Holocene Santa Monica
1083 Basin, California: Implications for evaluating source-to-sink flux at millennial time
1084 scales: Geological Society of America Bulletin, v. 121, p. 1394-1408.

1085 Russell, A.J., and Arnott, R.W.C., 2003, Hydraulic-jump and hyperconcentrated-flow
1086 deposits of a glacigenic subaqueous fan: Oak Ridges Moraine, Southern Ontario,
1087 Canada: Journal of Sedimentary Research, v. 73, p. 887-905.

1088 Sala, M., and Long, B.F., 1989, Évolution des structures deltaïques du delta de la rivière
1089 Natashquan, Québec: Géographie physique et Quaternaire, v. 43, p. 311-323.

1090 Shaw, J., Gareau, P., and Courtney, R.C., 2002, Palaeogeography of Atlantic Canada 13-
1091 0 kyr: Quaternary Science Reviews, v. 21, p. 1861-1878.

1092 Shaw, J., Piper, D.J.W., Fader, G.B.J., King, E.L., Todd, B.J., Bell, T., Batterson, M.J.,
1093 and Liverman, D.G.E., 2006, A conceptual model of the deglaciation of Atlantic
1094 Canada: Quaternary Science Reviews, v. 25, p. 2059-2081.

1095 Smith, N.D., Phillips, A.C., and Powell, R.D., 1990, Tidal drawdown: a mechanism for
1096 producing cyclic sediment laminations in glaciomarine deltas: Geology, v. 18, p. 10-
1097 13.

1098 St-Onge, G., Lajeunesse, P., Duchesne, M.J., and Gagné, H., 2008, Identification and
1099 dating of a key Late Pleistocene stratigraphic unit in the St. Lawrence Estuary and
1100 Gulf (Eastern Canada): Quaternary Science Reviews, v. 27, p. 2390-2400.

St-Onge, G., and Long, B.F., 2009, CAT-scan analysis of sedimentary sequences: An ultrahigh-resolution paleoclimatic tool: Engineering Geology, v. 103, p. 127-133.

St-Onge, G., Mulder, T., Francus, P., and Long, B., 2007, Continuous Physical Properties of Cored Marine Sediments, *in* Hillaire-Marcel, C., and De Vernal, A., eds, Proxies in Late Cenozoic Paleoceanography: Development in Marine Geology 1, p. 63-98.

St-Onge, G., Mulder, T., Piper, D.J.W., Hillaire-Marcel, C., and Stoner, J.S., 2004, Earthquake and flood-induced turbidites in the Saguenay Fjord (Québec): a Holocene paleoseismicity record: Quaternary Science Reviews, v. 23, p. 283-294.

St-Onge, G., Stoner, J.S., and Hillaire-Marcel, C., 2003, Holocene paleomagnetic records from the St. Lawrence Estuary, eastern Canada: centennial- to millennial-scale geomagnetic modulation of cosmogenic isotopes: Earth and Planetary Science Letters, v. 209, p. 113-130.

Stuiver, M., and Reimer, P.J., 1993, Extended 14C Data Base and Revised Calib 3.0 14C Age Calibration Program: Radiocarbon, v. 35, p. 215-230.

Sumner, E.J., Amy, L.A., and Talling, P.J., 2008, Deposit Structure and Processes of Sand Deposition from Decelerating Sediment Suspensions: Journal of Sedimentary Research, v. 78, p. 529-547.

Swenson, J.B., Paola, C., Pratson, L., Voller, V.R., and Murray, A.B., 2005, Fluvial and marine controls on combined subaerial and subaqueous delta progradation:

Morphodynamic modeling of compound clinoform development: Journal of Geophysical Research: Earth Surface, v. 110, doi: 10.1029/2004JF000265.

Syvitski, J.P.M., and Praeg, D., 1989, Quaternary Sedimentation in the St. Lawrence Estuary and Adjoining Areas, Eastern Canada: An Overview Based on High-Resolution Seismo-Stratigraphy: Géographie physique et Quaternaire, v. 43, p. 291-310.

Talling, P.J., 2014, On the triggers, resulting flow types and frequencies of subaqueous sediment density flows in different settings: Marine Geology, v. 352, p. 155-182.

Talling, P.J., Masson, D.G., Sumner, E.J., and Malgesini, G., 2012, Subaqueous sediment density flows: Depositional processes and deposit types: Sedimentology, v. 59, p. 1937-2003.

Tarasov, L., Dyke, A.S., Neal, R.M., and Peltier, W.R., 2012, A data-calibrated distribution of deglacial chronologies for the North American ice complex from glaciological modeling: Earth and Planetary Science Letters, v. 315-316, p. 30-40.

Warrick, J.A., Simms, A.R., Ritchie, A., Steel, E., Dartnell, P., Conrad, J.E., and Finlayson, D.P., 2013, Hyperpycnal plume-derived fans in the Santa Barbara Channel, California: Geophysical Research Letters, v. 40, p. 2081-2086.

FIGURES

Figure 1 : Location of study area and main locations of submarine canyons and fans mentioned in the text. RC = River-fed canyon, LDC = Longshore drift-fed canyons, RDC = River-fed deltaic channels, SSC = Sediment-starved canyons

Figure 2 : Deglaciation of the Québec North Shore (modified from Occhietti et al., 2011) with the extent of three watersheds discussed in the text as well as the relative sea-level curves for the Lower St. Lawrence Estuary. (A) is from Dietrich et al. (in press) and (B) is from Dionne (2001).

Figure 3 : Seismic stratigraphic framework of the Lower St. Lawrence Estuary illustrating the five main seismic units and their ages (modified from Duchesne et al., 2010). Location of seismic profile in Fig. 1. Depths were converted from time using a velocity of 1500 m/s.

Figure 4: A) Stratigraphic architecture of a modern exposed component of the deltaic system (Portneuf) showing the lateral juxtaposition, from the proximal to distal domain of outwash fan, glaciofluvial delta and coastal suites. Letters within the sketch represents the inserts; B) faint horizontal bedding in pebbles and cobbles and sand intraclasts forming the topsets of the outwash fan; C) stacked normally-graded beds deposited from sediment density flows; D) boulder-sized lonestone in glaciomarine mud; E) trough cross-stratified sand and gravel in delta topsets; F) stacked normally graded and flamed sand beds deposited by sediment density flows, forming the bulk of the glaciofluvial delta slope; G) well-bedded silt deposits forming the prodelta; H) well-sorted sand and heavy mineral placers observed in raised beach deposits, note vertical burrows; I) seaward-dipping beds characterizing the raised beaches and spits.

Figure 5: Bathymetry of the submarine deltas and fans discussed in the text. A) The Portneuf delta illustrating buried channels at the mouth of the river and the prevalence of longshore drift landforms (spit) in the nearshore environment; B) The Manicouagan delta illustrating channels at the mouth of the river; C) The Les Escoumins region illustrating a river-fed submarine canyon to the West and three longshore drift-fed submarine canyons to the East.

Figure 6: Seismic stratigraphy of the (A) submarine Portneuf delta, (B) submarine Manicouagan delta, (C) Les Escoumins river-fed canyon/fan system and (D) Les Escoumins longshore drift-fed canyon/fan system. In all four cases, the main submarine fan units overly transparent to low-amplitude seismic reflections (SU3). The Portneuf submarine fan (A) is overlied by transparent to low-amplitude seismic reflections (SU3) and late-Holocene sediments (SU4 and SU5) while the Manicouagan submarine fan (B) is overlied by low amplitude seismic reflections (SU5: postglacial hemipelagic sediments). Location of seismic profiles in Fig. 5. Depths were converted from time using a velocity of 1500 m/s.

Figure 7: Distribution of sediment density flow deposits (hyperpycnite-like deposits (H)) in the Manicouagan delta, characterized by sharp increases in CT-numbers and magnetic susceptibility. A, B, C and D are cores collected on the submarine delta (location in Fig. 5B). E) Examples of grain-size patterns observed within the cores illustrating inverse-to-normal grading and more complex grading patterns similar to hyperpycnites.

Figure 8: Distribution of sediment density flow deposits (debrites (D) and turbidites (T)) in the river-fed (A) and longshore drift-fed (B) submarine fans of the Les Escoumins

1183 sector. C) Thin section of turbidites illustrating the normal-grading and basal inverse-
1184 grading interpreted as the traction carpet.

1185 **Figure 9:** Conceptual model of evolution of deltaic system and submarine fans in the
1186 LSLE following the retreat of the Laurentide Ice Sheet (LIS) margin. Phase 1 is
1187 characterized by a retreating ice-margin on the Québec North Shore and the progradation
1188 of a delta over the shelf (formation of outwash fans and progradation of glaciofluvial
1189 deltas) during RSL fall. Phase 2 is characterized by the delivery of sediment into the
1190 Laurentian Channel during the early-Holocene while the LIS is still present in the upper
1191 parts of the river watersheds. Phase 3 is characterized by the complete withdrawal of the
1192 LIS from the watersheds and the erosion of the deltas, the development of extensive
1193 coastal structures on the shelf and the activity of the Les Escoumins longshore drift-fed
1194 systems during the mid- to late-Holocene.

1195 **Table 1** : AMS ^{14}C dates and calibrated ages for submarine samples collected in the
1196 LSLE. A marine reservoir correction of 400 yr (ΔR – 0 yr using Marine 13 curve) was
1197 applied and calibrated ages within parentheses presented with 2σ.

Figure 1

Click here to download Figure Fig-1_loc.tif

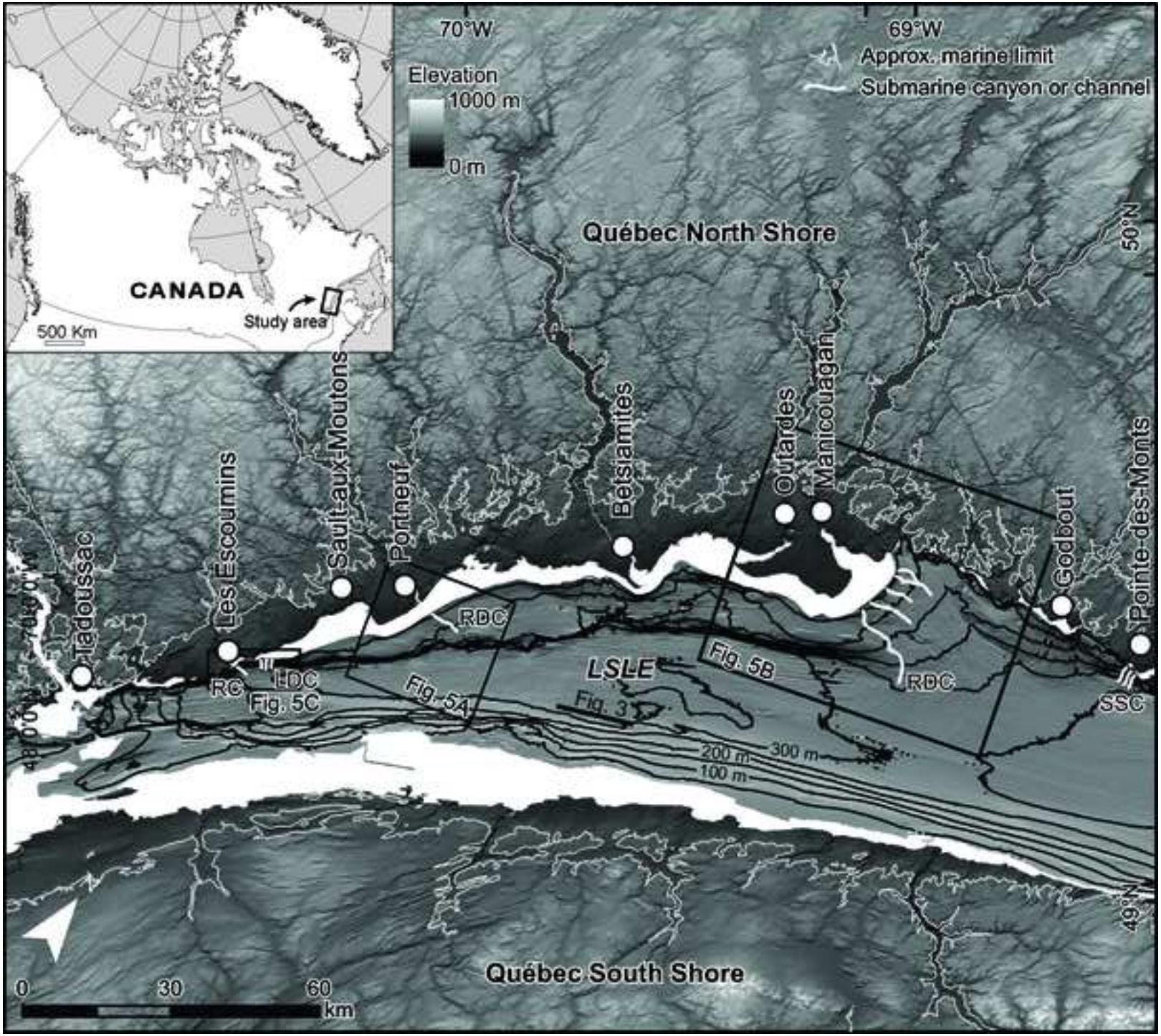

Figure 2

Click here to download Figure Fig-2.tif

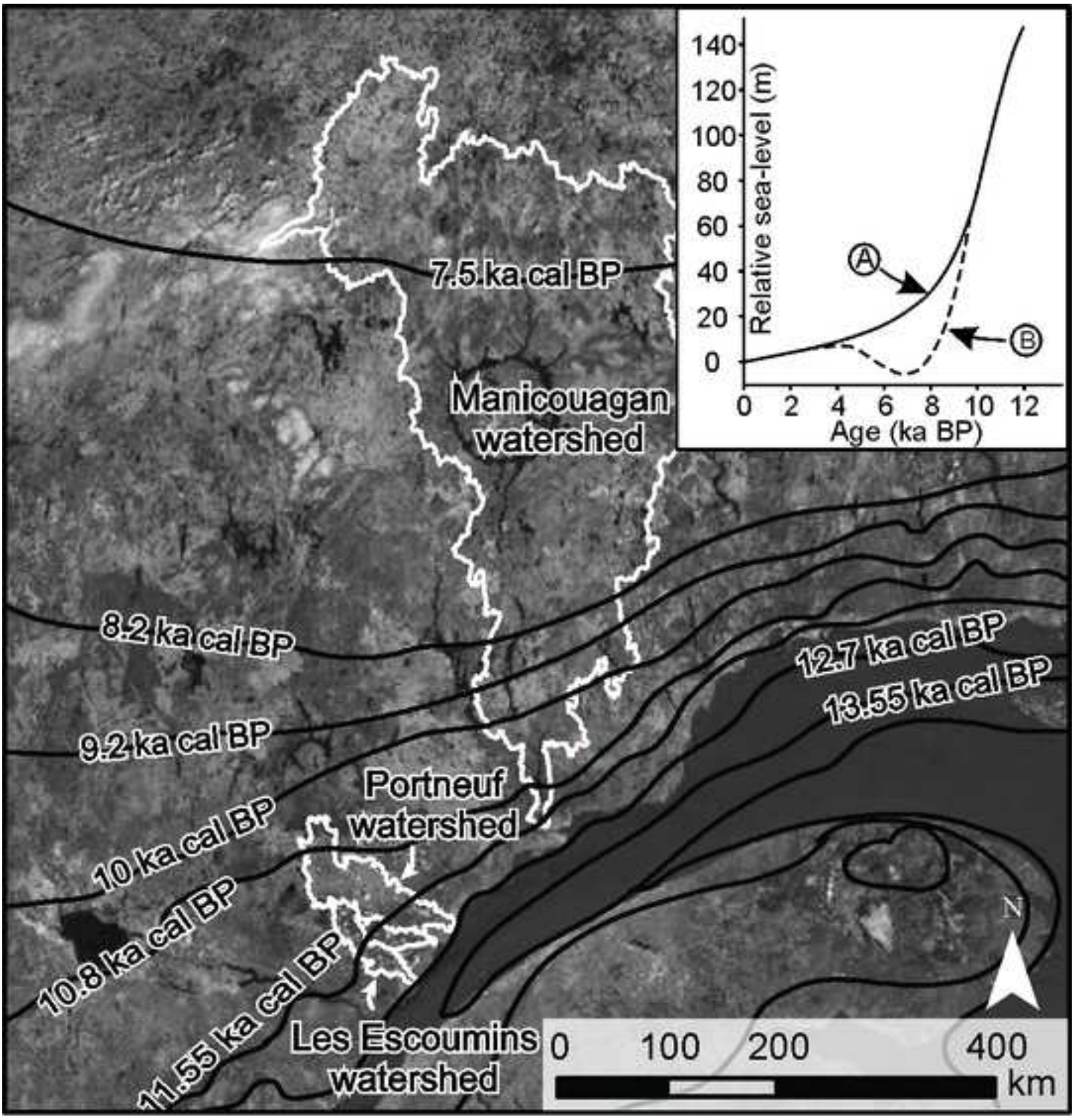

Figure 3

Click here to download Figure Fig-3.tif

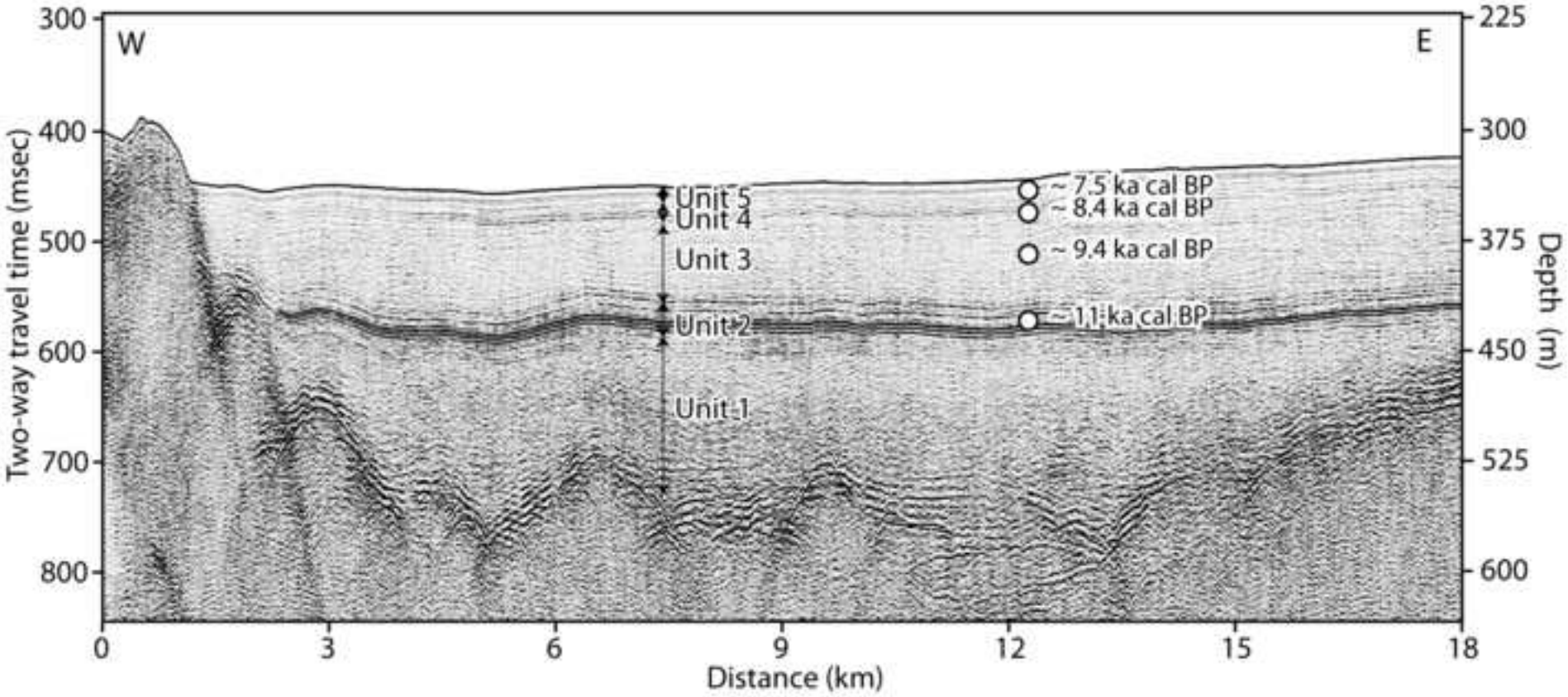

Figure 4

Click here to download Figure Fig-4.tif

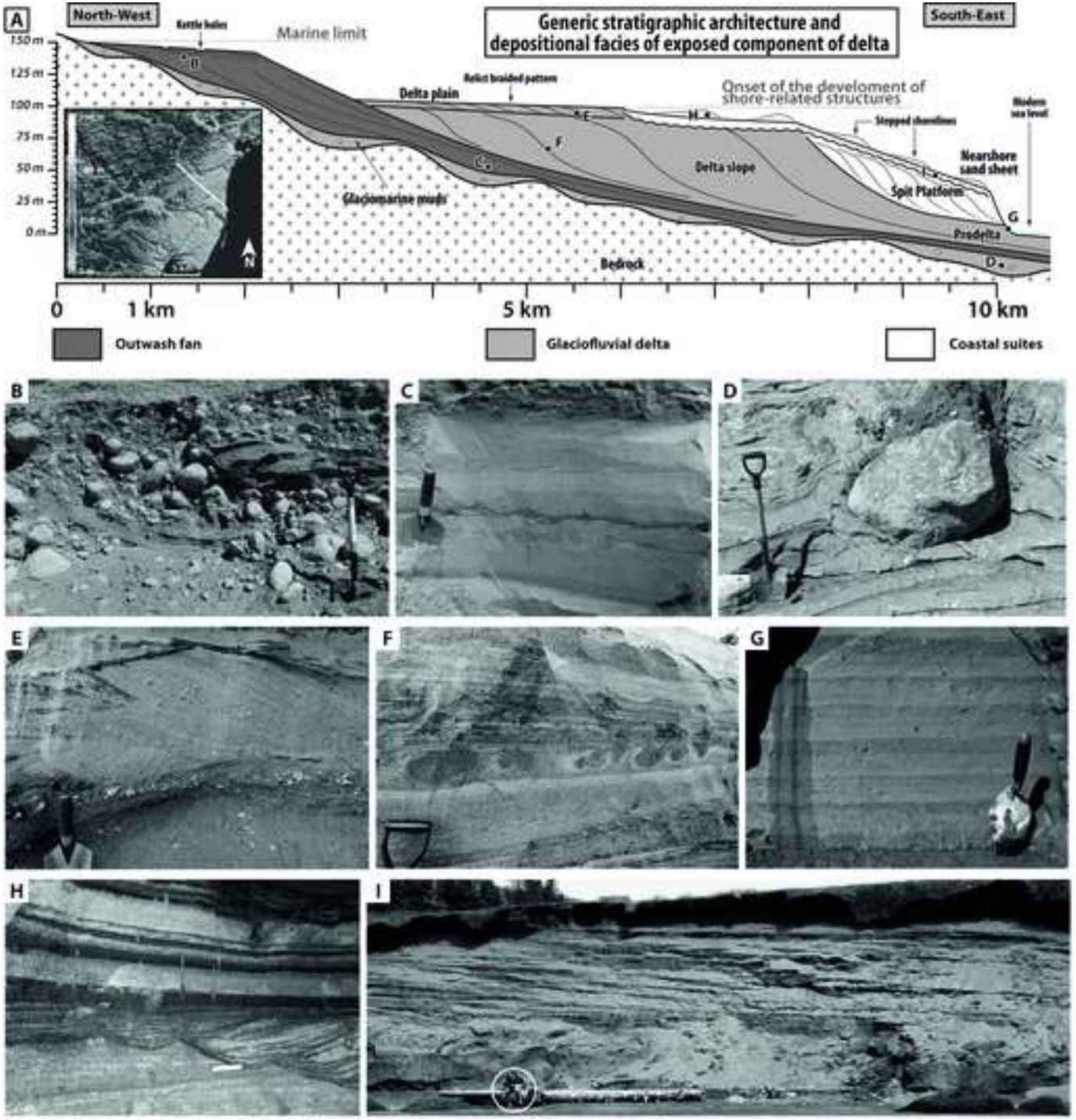

Figure 5

Click here to download Figure Fig-5_bathy.tif

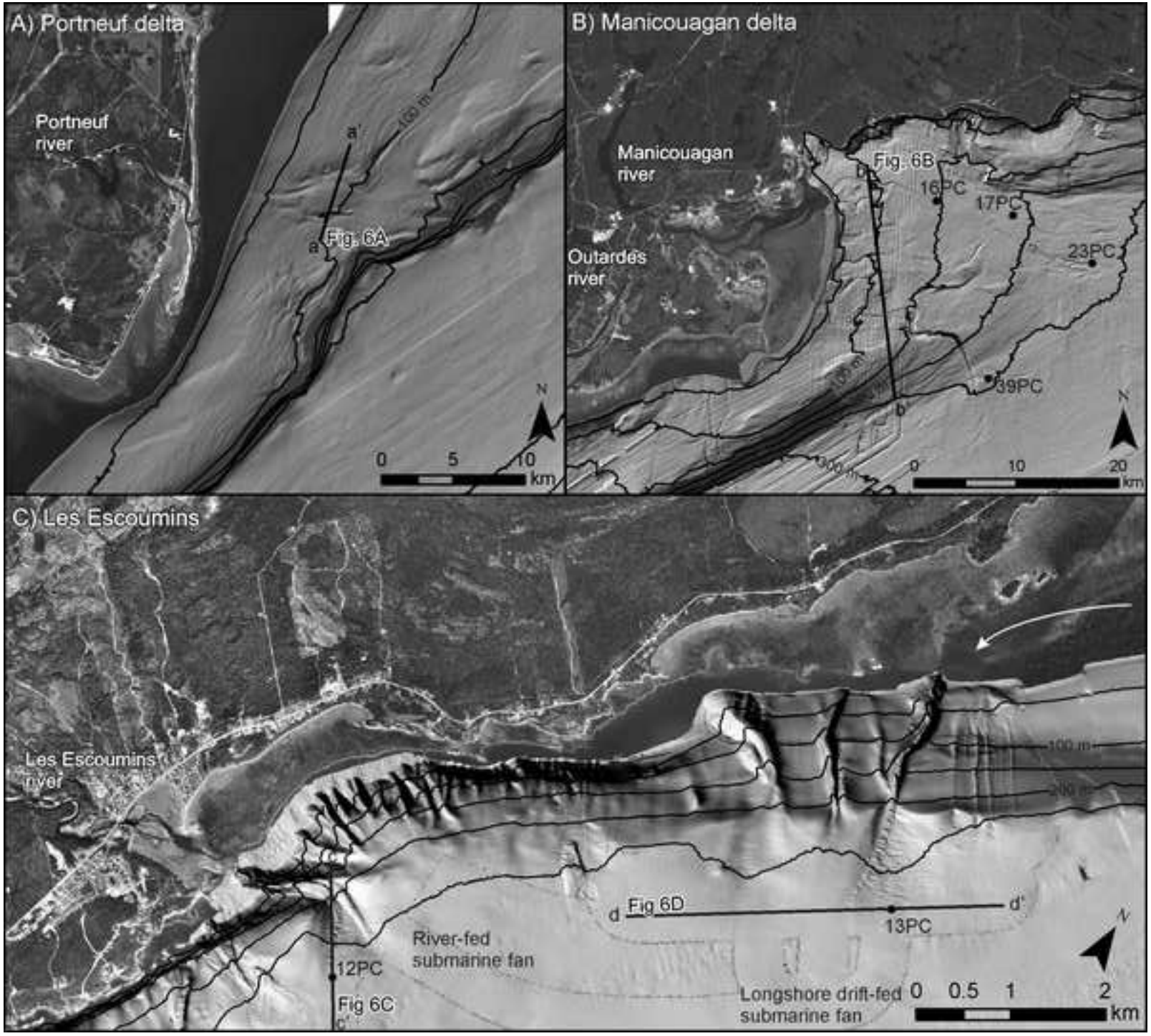

Figure 6

Click here to download Figure Fig-6_sismique.tif

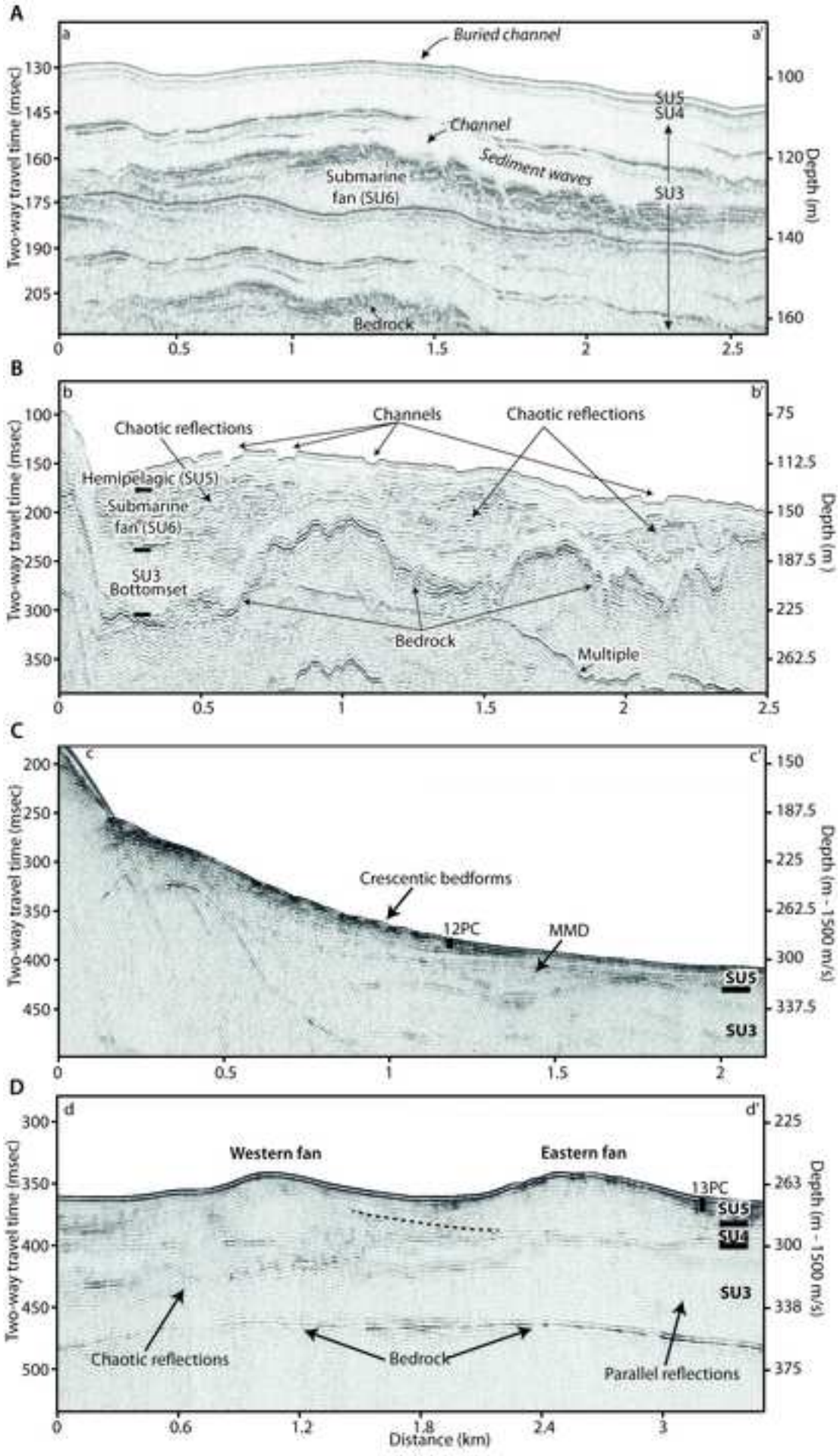

Figure 7

Click here to download Figure Fig-7.tif

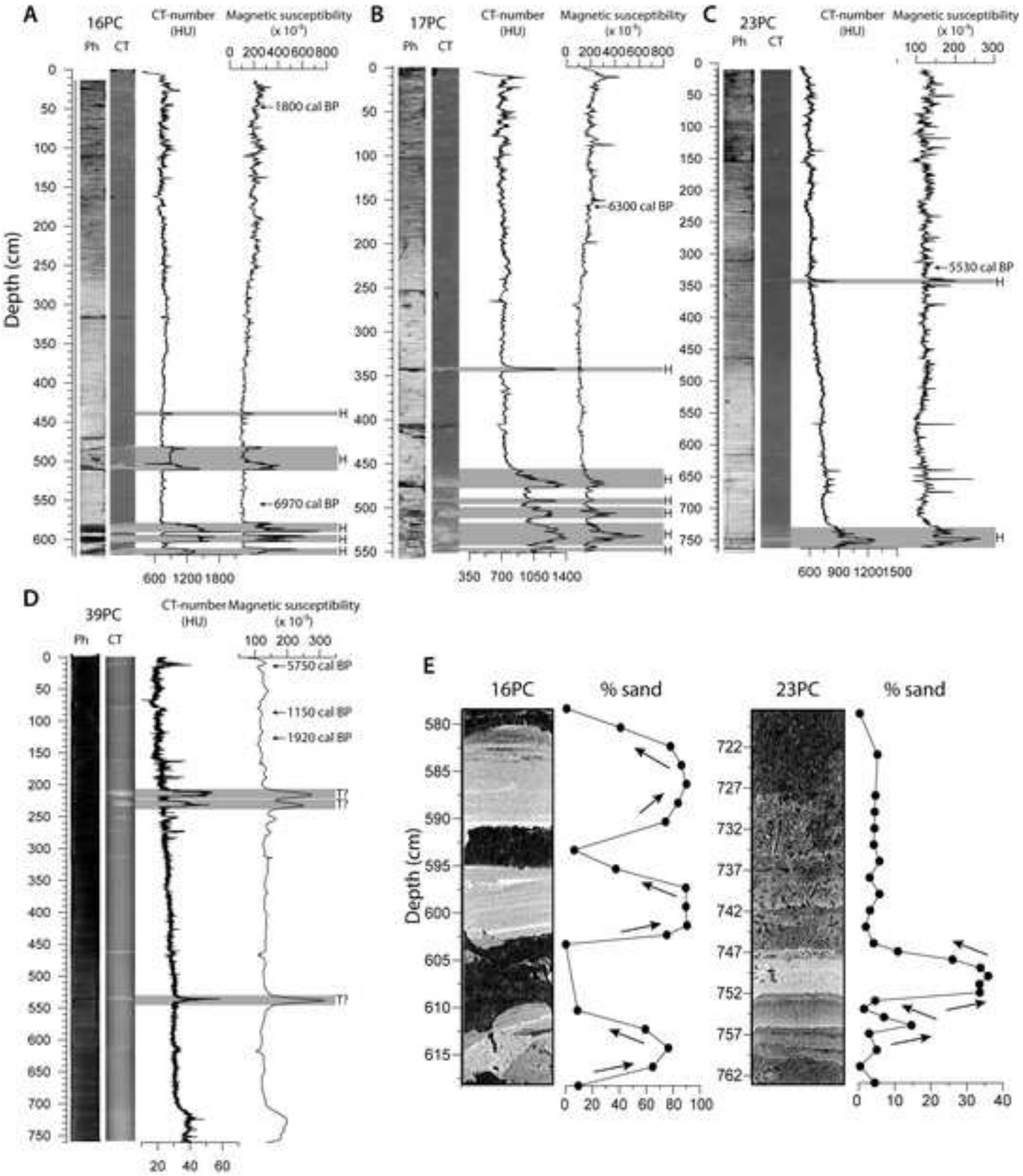

Figure 8

Click here to download Figure Fig-8.tif

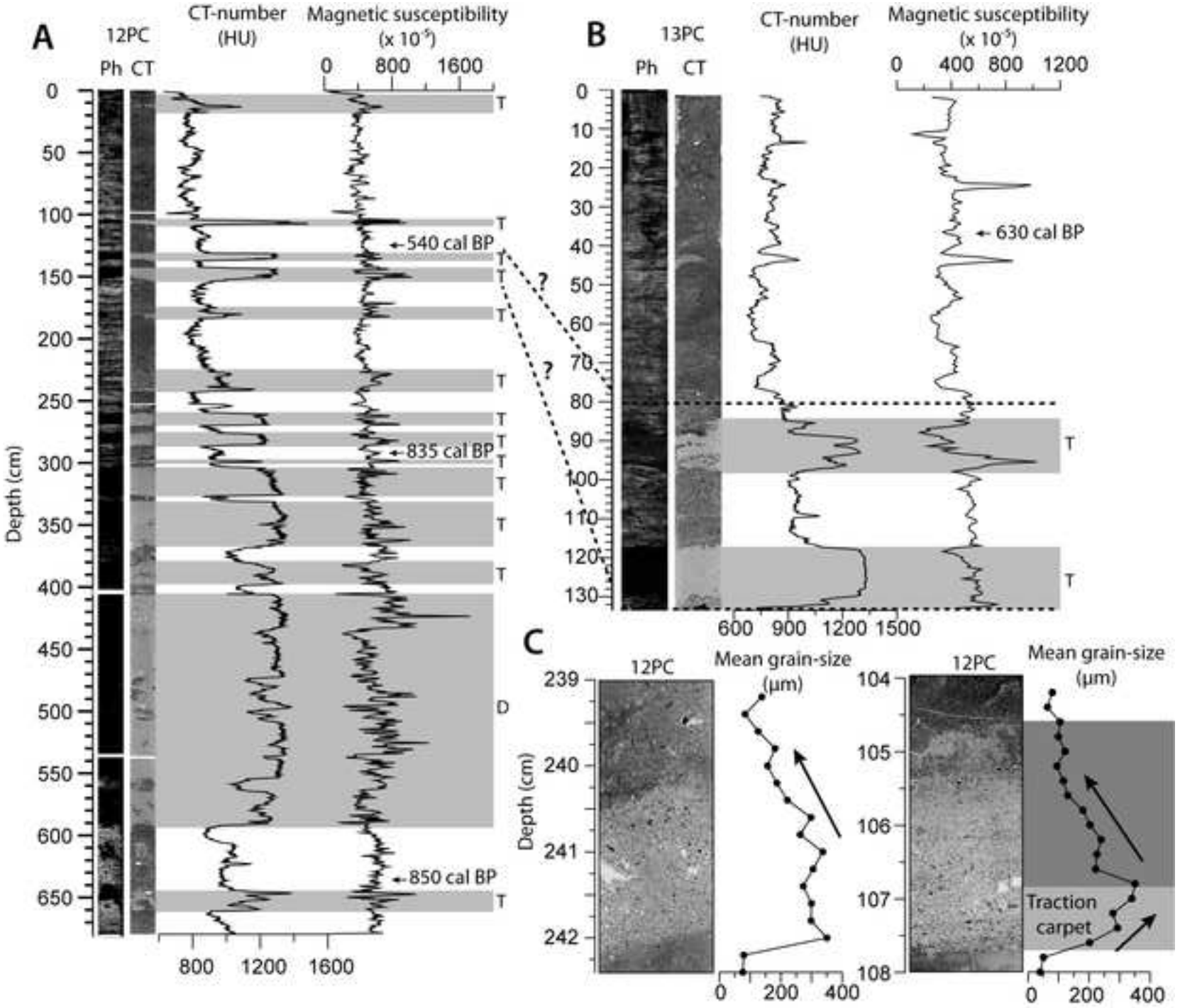

Figure 9

Click here to download Figure Fig-9_synthese.tif

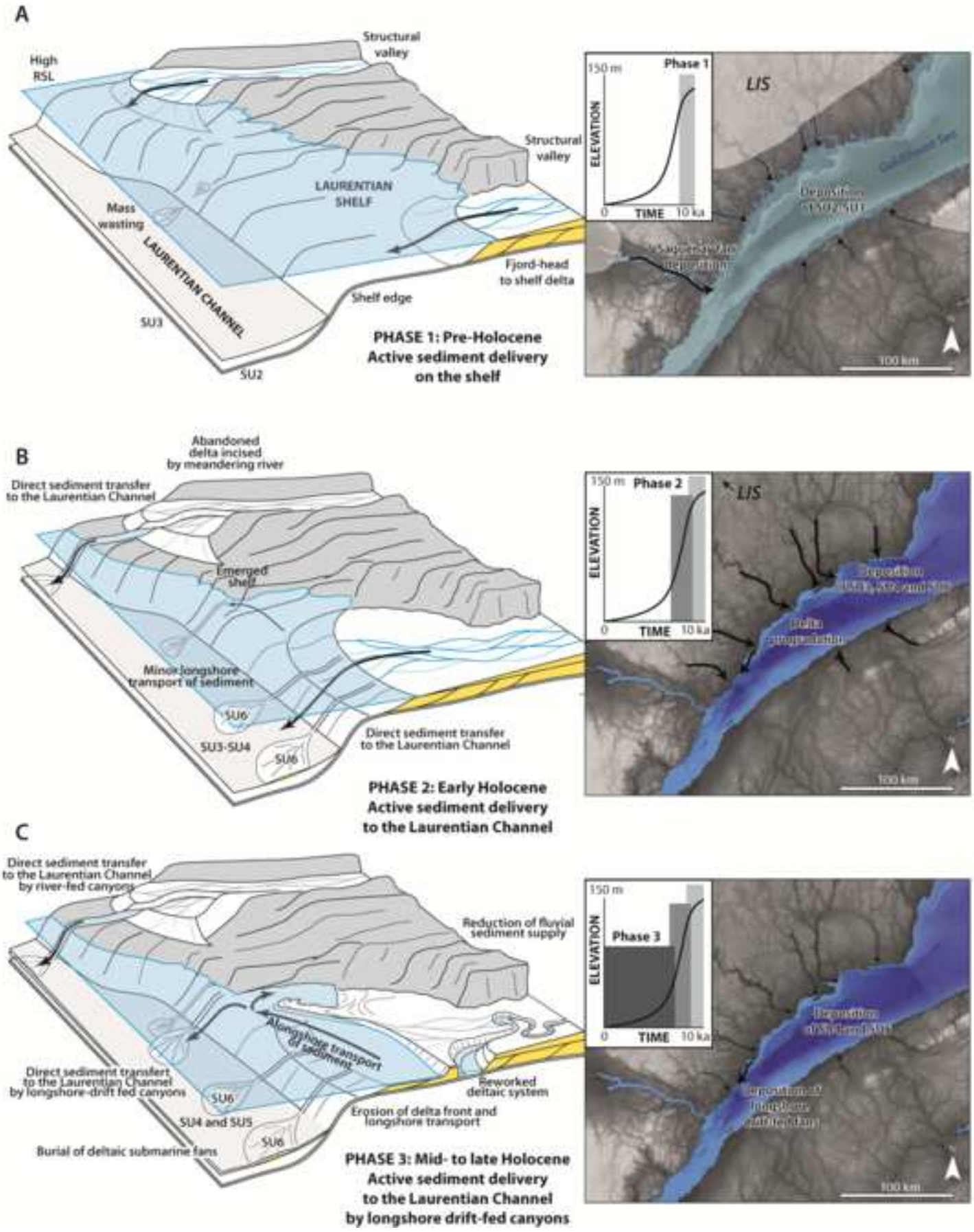

Table 1

Core number	Depth in core (cm)	^{14}C Age (yr BP)	Calibrated age (cal BP)	Dated material	Laboratory number
COR0602-39PC	8	5390 ± 80	5750 (5588 - 5913)	Shell fragment	TO-13204
COR0602-39PC	91	1590 ± 50	1150 (1032 - 1266)	Shell fragment	TO-13205
COR0602-39PC	126	2300 ± 50	1920 (1786 - 2055)	Shell fragment	TO-13206
COR1203-12PC	117	930 ± 15	540 (578 - 594)	Shell fragment	UCIAMS-127440
COR1203-12PC	291	1285 ± 15	835 (769 - 897)	Wood	UCIAMS-127422
COR1203-12PC	644	1310 ± 20	850 (785 - 914)	Organic matter	UCIAMS-127421
COR1203-13PC	35	1060 ± 15	630 (590 - 667)	Shell fragment	UCIAMS-127438
COR1203-16PC	41	2205 ± 15	1800 (1727 - 1868)	Shell fragment	UCIAMS-127443
COR1203-16PC	561	6470 ± 20	6970 (6880 - 7059)	Organic matter	UCIAMS-127426
COR1203-17PC	170	5875 ± 25	6300 (6224 - 6373)	Shell fragment	UCIAMS-127454
COR1203-18PC	115	4655 ± 15	4880 (4820 - 4941)	Shell fragment	UCIAMS-127453
COR1203-23PC	324	5180 ± 20	5530 (5472 - 5589)	Shell fragment	UCIAMS-127444